MEASUREMENT AND THEORETICAL TREATMENT OF THE COLLOIDAL FORCES ACTING ON A MODEL COLLOID

- SHEAR INDUCED AGGREGATION

AUTHOR : JANET PRESTON

SUPERVISOR : DR. G.P. MATTHEWS

BSc. COMBINED HONOURS COURSE

MAY 1992

1. ABSTRACT

Consideration of theoretical aspects of colloid stability suggests that shear induced collisions may lead to prolonged or permanent aggregation of particles, providing that the hydrodynamic compressive force between the colliding particles supasses their repulsive force. By equating the hydrodynamic compressive force to the repulsive force, the critical shear rate for shear induced aggregation of a model colloid can be predicted.

The theoretical model was compared to experimental data obtained by shearing a suspension of the model polystyrene latex on a Bohlin VOR rheometer. The mean particle size of the sheared latex was measured using Photon Correlation Spectroscopy (PCS), which allowed detection of the onset of particle aggregation. Shearing of a sample of Lytron 2503, a commercially available polystyrene latex, did not result in any detectable particle aggregation. However the repulsive force barrier was calculated to be greater than the hydrodynamic forces incurred by shearing.

Addition of 1:1 electrolyte enabled the repulsive force barrier between particles to be lowered sufficiently so as to equal the hydrodynamic forces incurred. The calculated critical shear rate for shear induced aggregation correlated well with the shear rate at which aggregation was detected experimentally.

3. INTRODUCTION

Styrene copolymer latices have been used for many years in the paper industry as binders. Many and varied types of latex are available, for example styrene/butadiene and styrene/acrylic copolymers are extensively used.

The latices are mixed with mineral slurries and other additives such as flow modifiers to form a "coating colour", and are used to 'glue' the mineral particles both to each other and to the base paper. A typical coating colour formulation might consist of the following ingredients:

100 parts dry weight clay
0.3 " Dispex N40 (a polyacrylate dispersant)
0.1 " NaOH
1.0 " Na carboxy-methyl cellulose (a flow modifier)
11 " Latex
Water to give final solids ~ 60%

All parts referred to by weight based on 100 parts clay.

Plates 1 and 2 are scanning electron micrographs of coating colour which has been freeze fractured (1,2). The latex particles can be seen dispersed amongst the clay platelets. On heating the latex particles coalesce to form a film which binds the clay particles to the surface of the paper.

The size and shape of the particles have a profound effect on the flow properties of the colour and hence on the structure of the coating itself. In the head of a blade coater, anisotropic pigment particles need to align to enable them to pass smoothly under the blade onto the paper. Aggregation of coating colour constituents will cause disruption of the colour flow under the blade and will produce a coating which will appear rough and uneven (Figure 1). Visual assessment of the coating surface will show areas of 'spits of dry colour' and 'streaks of uncoated paper'. The high speeds used in modern coating mills, up to 1500 m min^{-1}, accentuate this problem causing "runnability" to be a prime consideration.

Figure 1. Runnability Problems in a Coating Head

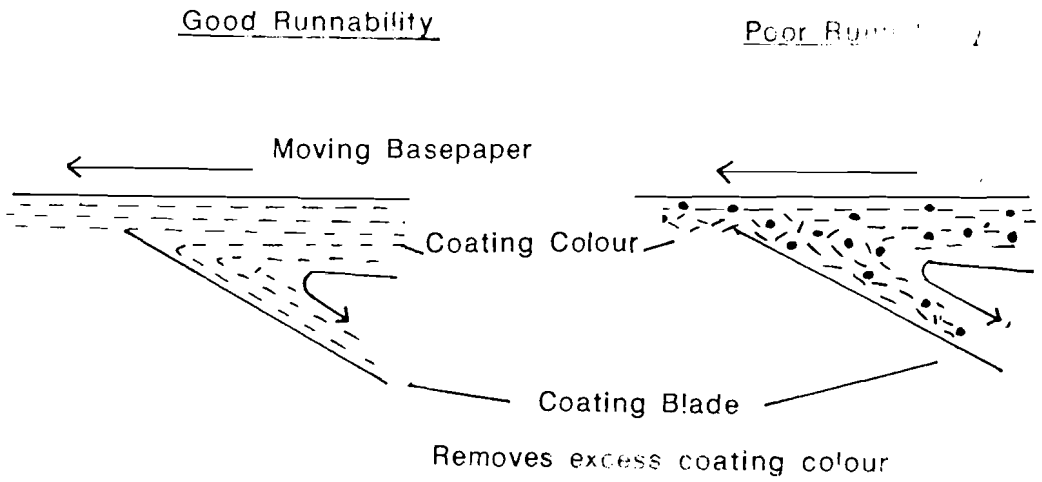

The combination of large platey particles and small blocky particles such as aggregates will also affect the finished sheet properties. A disordered coating will give the paper a bright appearance due to light being scattered but a low gloss (Figure 2).

Figure 2. Particle Alignment on a paper surface - gloss and light scattering.

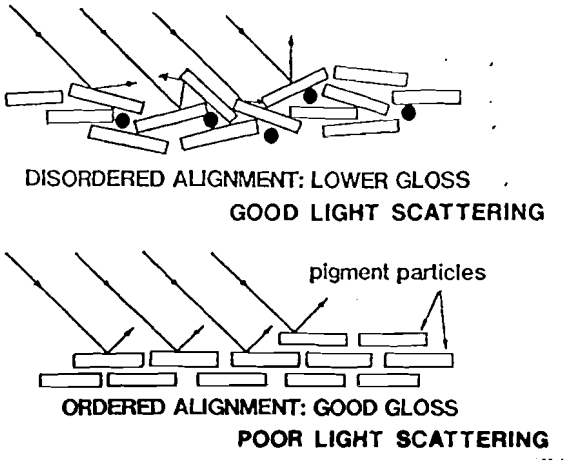

There is evidence from the literature (3,4) to suggest that aggregation of latex particles can occur under high shear conditions. Any such aggregation in the colour would have a significant effect upon the paper coating and the final sheet properties. This study seeks to consider the theoretical aspects

of colloid stability and study the effect of shear upon a model colloid. Polystyrene latex was chosen as the model because it can be characterised readily and was similar in surface chemistry to paper coating latices.

The coating colour is subjected to high shear rates (approx. 10^6 / s^{-1}) as it passes from the coating head to the paper under a blade. A Bohlin VOR rheometer was used in this study to apply the shear to the latex. Samples of latex were subjected to a single predetermined shear rate for a fixed time before being recovered. The sample was then diluted and its mean particle size measured using Photon Correlation Spectroscopy (PCS). In an attempt to understand the critical factors involved in the aggregation, theoretical calculations were made of the forces involved. The repulsive force barrier between a pair of particles was calculated using the Derjaguin, Landau, Verwey and Overbeek (DLVO) theory of colloid stability (5) and was compared with the hydrodynamic force resulting from fluid flow, using an equation derived by Goren (6). The shear rate at which the hydrodynamic force just exceeds the DLVO repulsive barrier height was used to predict the onset of aggregation, and was called the critical shear rate.

LATEX PREPARATION - EMULSION POLYMERISATION

Latices used in the paper coating industry are prepared by emulsion polymerisation. Polystyrene preparation involves four basic ingredients; styrene monomer, water, emulsifier and a free radical initiator (7). The mechanism is described below:

When surface active agents or 'surfactants' are dissolved in water in concentrations above a critical level, they associate with one another to form tiny uniform spheres or micelles. In a micelle the surfactant molecules are arranged with their hydrophobic tails pointing inwards and their hydrophilic heads pointing towards the water. Surfactants such as sodium dodecyl sulphate are used and can be represented as

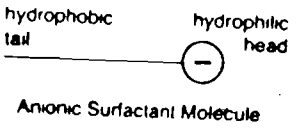

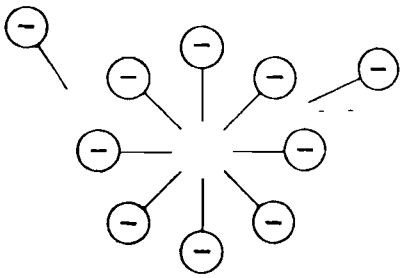

a micelle

The micelles contain an optimum number of surfactant molecules and so are monosized or monodispersed. Addition of more surfactant molecules results in the formation of extra micelles of exactly the same size. When styrene monomer is added it is found in three loci, dissolved in the aqueous phase, in the emulsion droplets and solubilised in the micelles.

A water soluble polymerisation initiator is then added to the system e.g. potassium persulphate. Upon heating the persulphate ion decomposes into two sulphate ion free radicals.

$$S_2O_8^{2-} \dashrightarrow 2\ SO_4^{-}.$$

This first stage of emulsion polymerisation is known as initiation, the reactions and corresponding rate equations can be expressed as follows (8):

$$I \xrightarrow{k_d} 2R^* \qquad \ldots\ldots (1)$$

$$R^* + M \xrightarrow{k_i} RM^* \qquad \ldots\ldots (2)$$

In most polymerisations the second step (the addition of the primary radical to monomer) is much faster than the first step. The homolysis of the initiator is the rate determining step in the initiation sequence and the rate of initiation is then given by:

$$R_i = 2\ f\ k_d\ [I] \qquad \ldots\ldots\ (3)$$

where I = initiator
R* = free radical
RM* = radical generated by reaction with monomer M
k_d = decomposition rate constant of the initiator
R_i = the rate of initiation
f = the efficiency factor which accounts for the fact that not all radicals produced in reaction 1 initiate polymerisation.
k_i = rate constant for initiation
M = monomer

For redox initiator systems usually used for low temperature emulsion polymerisation e.g. potassium persulphate, the rate of initiation is as follows:

$$R_i = k_i\ [\text{oxidant}]\ [\text{reductant}] \qquad \ldots\ldots\ (4)$$

The free radicals migrate from the aqueous phase and adsorb onto the surface of swollen micelles to initiate polymerisation. This stage is known as "propagation" and can be expressed by the following equations:

$$RM^* + M \xrightarrow{k_p} RMM^* \xrightarrow{k_p} R^*_n \qquad \ldots\ldots\ (5)$$

$$R_p = k_p\ [R_n^*]\ [M] \qquad \ldots\ldots\ (6)$$

where k_p = the propagation rate constant
R_n^* = a macromolecular radical with n monomers
R_p = rate of propagation

The radicals continue to grow in the micelles until another radical enters and causes termination. "Termination" can be caused by the combination of 2 polymer radicals to form one polymer molecule or by disproportionation to form 2 polymer molecules:

$$R_n^* + R_m^* \xrightarrow{k_{tc}} P_{n+m} \qquad \ldots\ldots\ (7)$$

$$R_n^* + R_m^* \xrightarrow{k_{td}} P_n + P_m \qquad \ldots\ldots\ (8)$$

$$R_t = k_t [R^*]^2 \quad \ldots\ldots (9)$$

where R_t = rate of termination
k_t = termination rate constant
P = polymer molecules

One other type of reaction may occur during emulsion polymerisation known as a transfer reaction. A growing polymer radical may react with a large variety of molecules by abstracting a hydrogen or halogen atom from another compound to terminate itself and form a new radical. This new radical may react with other monomer molecules to form another polymer chain.

$$R_n^* + TX \xrightarrow{k_n} P_n X + T^* \quad \ldots\ldots (10)$$

where k_n = the transfer rate constant
TX = the transfer species
P_n = polymer
T* = the transfer radical

Transfer reactions may lead to the formation of branched or crosslinked polymers.

Thus the monomer swollen micelle is transformed into a monomer swollen polymer particle of much greater size. As monomer is consumed in the polymerisation more diffuses from the droplets through the aqueous phase to the site of polymerisation. This process proceeds until all of the micelles have disappeared either by capturing radicals and becoming polymer particles or by disbanding to give up their emulsifier to neighbouring micelles which have captured radicals. The polymer particles then continue to grow until the supply of monomer or radicals is exhausted.

The aqueous phase of the latex may contain emulsifier, residual initiator, its decomposition products and buffer. The latex particle surface may contain both physically adsorbed emulsifier molecules and chemically bound emulsifier groups (i.e. the sulphate groups) as well as other groups formed in side reactions such as carboxyls. There are several possible reasons for the formation of surface carboxyl groups, which can be summarised as follows (9):

1. hydrolysis of sulphate groups followed by oxidation.
2. dissolution of carbon dioxide in the latex
3. oxidation of surface sulphate groups, particularly in the presence of small concentrations of heavy metal ions
4. side reactions of initiating species.

Extra carboxyl groups are often incorporated into paper coating latices as they impart several useful properties to the latex, including enhanced mechanical and chemical stability, enhanced tolerance to the addition of mineral fillers, and greater ease of redispersion after drying.(10) These carboxyl groups are incorporated by the addition of unsaturated carboxylic acids (e.g. acrylic acid) which then polymerise onto the latex particle surface.

If the emulsifier and inorganic salts were removed from the aqueous phase and particle surface, the result would be a system of monodispersed particles stabilised only by chemically bound emulsifier groups. If the number of these chemically bound groups were determined, the result would form an ideal model for colloidal studies i.e. monodispersed spheres with a constant known surface charge density.

Figure 3. Schematic representation of emulsion polymerisation.

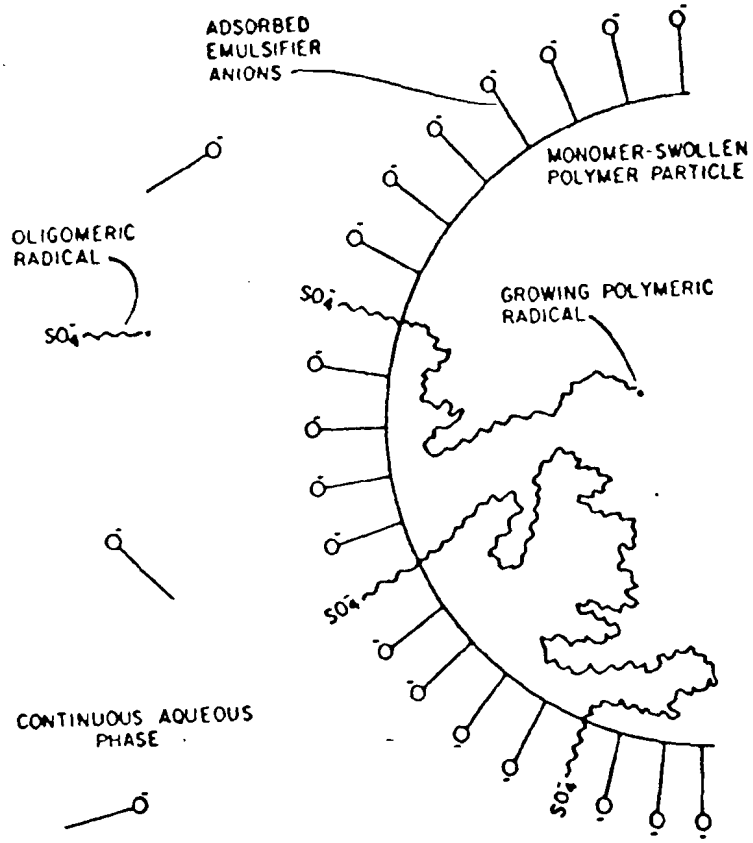

4.2. DOUBLE LAYER THEORY - COLLOID STABILITY

Dispersions of solid particles in a liquid media are considered to be colloidal if the particles are of such a size that they can be kept in suspension by the action of Brownian motion alone. This definition can be quantified by formulating the Peclet number appropriate to sedimentation, which for spherical particles is given by:

$$Pe = 6\pi a^4 \eta \Delta \rho g / kT \qquad \ldots\ldots\ldots (11)$$

where a = particle radius
$\Delta\rho$ = difference in density between solid and liquid phases
n = viscosity of medium
g = acceleration due to gravity
k = Boltzmann constant
T = Kelvin temperature

If $Pe < 1$ then thermal forces are expected to outweigh the force due to gravity. This is the case for most polymer latices (11).

In the colloidal state the discontinuous (solid) phase has a large area of contact with the continuous phase (liquid); consequently a large proportion of the atoms and molecules which make up the solid phase, experience some interaction with the liquid medium. This solid/liquid interaction has a significant effect on the total free energy of the system. Colloidal dispersions are therefore in general thermodynamically unstable, as processes such as coalescence or aggregation reduce the area of the solid phase in contact with the liquid and reduce the free energy of the system.

Stabilising factors are therefore incorporated in the latex during manufacture, and generally fall into 2 categories:

1. Electrostatic repulsions
   a) between ionised sulphate end groups which accumulate at the surface of the particles during manufacture
   b) between adsorbed or grafted surface active agents e.g. sodium dodecyl sulphate.
   c) between adsorbed or grafted polymeric species e.g. polycarboxylic acid chains.

2.Steric stabilisers such as hydrophilic macromolecules and non-ionic polymers which adsorb onto the latex.

Steric stabilisation is not applicable to Lytron 2503 and will not be considered in this study.

ATTRACTIVE FORCES

On a microscopic scale the thermodynamic instability of latex particles is manifest as a force of attraction. De Boer and Hamaker (12) were among the first to develop a quantitative theory, which involved summing the van der Waals interactions between pairs of atoms or molecules in each particle. More recently a general continuum theory of dispersion forces has been developed, in which the energy of interaction of 2 spherical particles at a separation 'H' can be found by:

$$V_A(H) = -\frac{A(H)}{12}\left[\frac{1}{Y} + \frac{1}{Y+1} + 2\ln\left[\frac{Y}{Y+1}\right]\right] \quad \ldots\ldots (12)$$

$$\text{Where } Y = \frac{H}{2a}\left[\frac{H+2}{2a}\right] \quad \ldots\ldots (13)$$

$$H = R - 2a \quad \ldots\ldots (14)$$

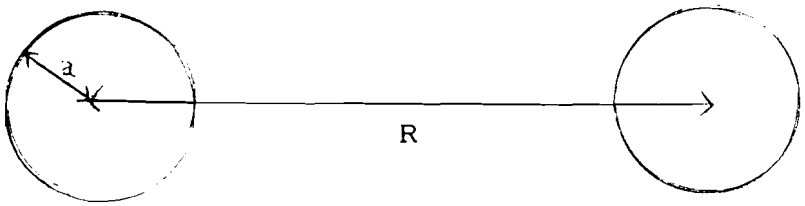

A = Hamaker function or coefficient and is a composite function of the material properties of particle and medium.

Colloid stability is largely influenced by the strength of the attraction at relatively close distances (R/2a ~ 1) and under these circumstances (12) has the form:

$$|V_A| < \frac{a\,A(H)}{12\,H} \quad \ldots\ldots (15)$$

This suggests that the van der Waals attraction should become significant compared to the thermal energy of two particles at room temperature, at separations of the order of 1/10 of a radius or less.

ELECTROSTATIC FORCES

The negatively charged sulphate and carboxyl groups which are on the surface of the latex, attract ions of the opposite charge which are called counter ions. The first layer of counter ions is called the Stern layer. Beyond the Stern layer is the diffuse layer which represents a steady falling off of the concentration of counter ions until the bulk of the solution is reached. Together these layers are known as the electrostatic double layer. An important property of the diffuse part of the double layer is its thickness and sensitivity to the presence of electrolyte in the aqueous medium. The extent of the diffuse layer can be assessed by considering the distribution of electric potential around a particle. The potential at a distance 'r' is given by:

$$\psi(r) \approx \psi(o) \quad \frac{a}{r} \quad \exp - \kappa (r-a) \qquad \ldots\ldots (16)$$

Where o = potential in the plane of the surface ion groups
ψ_0 = Debye - Huckel screening parameter
a = particle radius

κ is proportional to the square root of the ionic strength I and is given by

$$\kappa = \left[\frac{10^3 \, e^2 \, N_A}{\epsilon \, \epsilon o} \right]^{1/2} I^{1/2} \qquad \ldots\ldots (17)$$

(K is in m^{-1} and I is in mol dm^{-3})

where N_A = Avagadro's number
$\epsilon \, \epsilon o$ = absolute static permittivity of the medium
ϵo = permittivity of free space, 8.85×10^{-12} Fm^{-1}
The surface potential ψ_0 is related to the surface charge density and for small potentials (ψo << 50 mV)

$$\psi_o \sim \frac{\sigma_o a}{\epsilon \epsilon_o (1 + ka)} \quad \ldots\ldots (18)$$

where σ_o = surface charge density

The potential at distance 'r', $\psi(r)$ can be taken as a measure of the diffuse layer thickness.

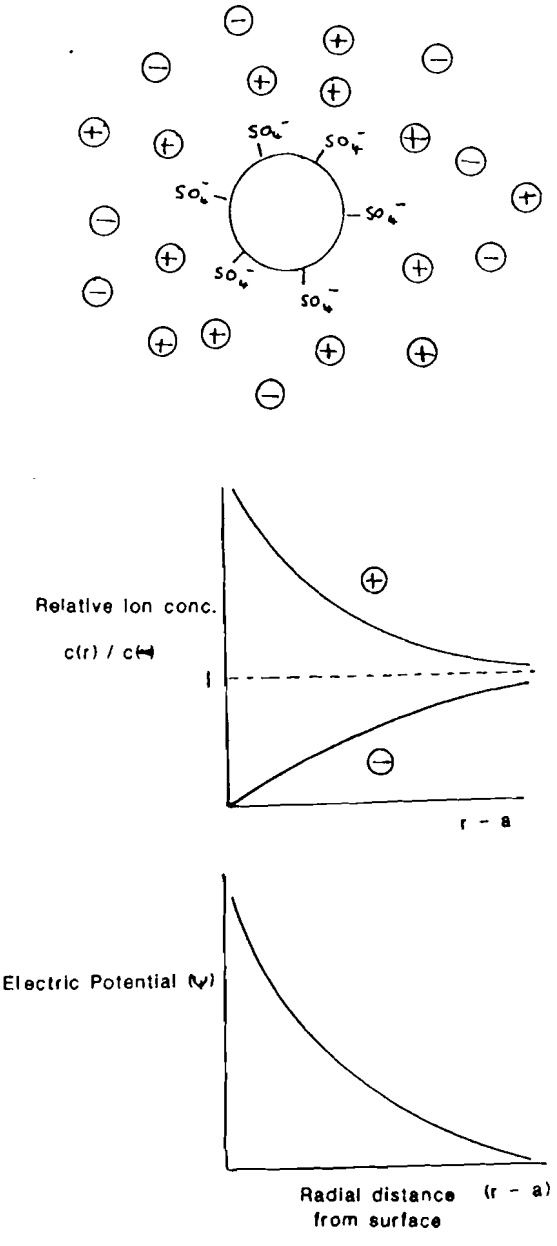

Figure 4. Potential distribution around a charged particle

POTENTIAL ENERGY CURVES AND STABILITY

The theory developed by Derjaguin, Landau, Verwey and Overbeek (DLVO theory) relates colloid stability to the total potential energy of interaction between a pair of particles i.e. $V = V_A + V_R$, (strictly speaking a short range repulsion representing particle contact should also be added.) Equations used in the DLVO calculation are summarised below:

$$V_R = 2 \pi \epsilon_o \epsilon_r a \psi_s^2 \cdot \frac{k \exp(-kH)}{1 + \exp(-kH)} \quad \text{for } ka > 10 \quad \ldots\ldots (19)$$

$$V_A = -\frac{Aa}{H^2}\left[\frac{4.90}{60\,P} - \frac{6.51}{180\,P^2} + \frac{2.36}{420\,P^3}\right] \quad \ldots\ldots (20)$$

and $$p = 2 \pi H / \lambda \quad \ldots\ldots (21)$$

$$\kappa^2 = 2 n_o V^2 e^2 / \epsilon_o \epsilon_r kT \quad \ldots\ldots (22)$$

$$V \text{ total} = V_R + V_A \quad \ldots\ldots (23)$$

Where V_R and V_A are repulsive and attractive forces respectively.

And where:

- ϵ_o = permittivity of free space
- ϵ_r = relative permittivity
- a = particle radius
- ψ_s = surface potential
- κ = Debye-Huckel reciprocal length
- H = interparticle separation
- A = combined Hamaker constant
- λ = dispersion length
- n_o = number of ions of each type
- V = valency of ions
- e = charge on electron
- k = Boltzmann constant

In this work the dispersion length was taken as 100 nm (13) and the combined Hamaker constant 1×10^{-20} J, an average value for polymer latices (14).

Under most circumstances the electrostatic repulsion outweighs the van der Waals attraction and give rise to a maximum in the curve at a distance of separation of 2 nm or so. The van der Waals attraction is, however, always dominant at closer distances of separation. The electrostatic repulsion can thus provide a barrier to particle contact. The total particle interaction between the colloidal particles is usually depicted as a potential energy - distance curve as shown in Figure 5a . The first derivative of the energy curve is a force curve which is shown in Figure 5b. The shapes of the curves and the height of the primary maximum V_{max} depend upon all the parameters which influence V_R and V_A. Important parameters are the surface potential, the ionic strength, the particle radius and the charge on the counter ion.

Surface Potential

A decrease in the surface potential of the latex will result in a decrease in the repulsive barrier height, e.g. for a particle of radius approx. 100 nm, an ionic strength of 10^{-3} mol dm^{-3} (1:1 electrolyte) and a Hamaker constant of 2 kT a series of curves could be produced (9):

Figure 6. Effect of Surface Potential on Potential Energy curves

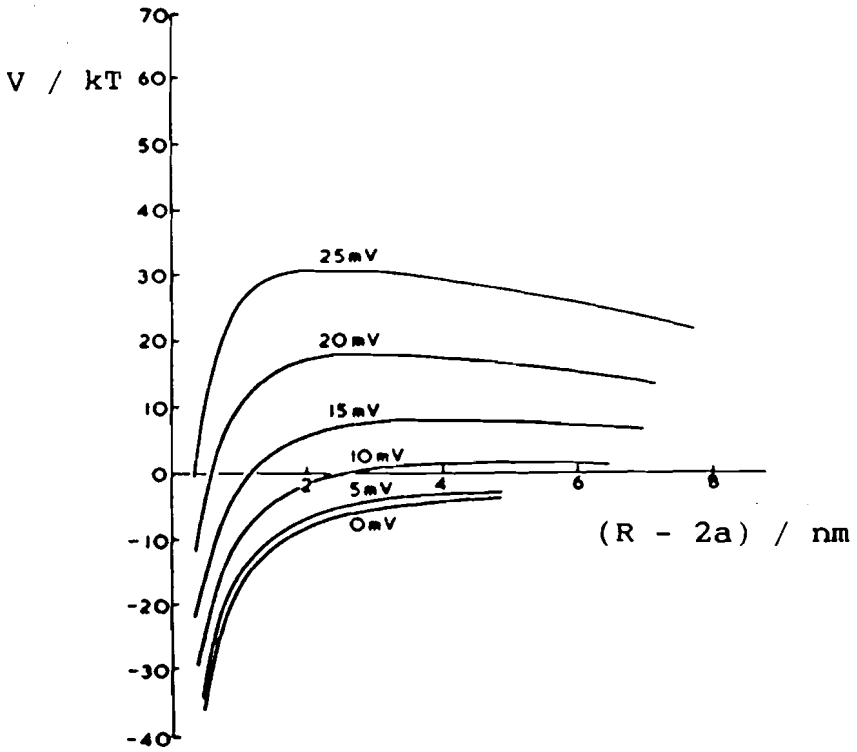

Potentials of approximately 20 mV are required to give a stable system (11).

Figure 7. Effect of Ionic Concentration

Increasing the electrolyte concentration also has the effect of depressing the repulsive force barrier, e.g. for the addition of 1:1 electrolyte to a system with particles of radius 100 nm and a surface potential of 30 mV, the following curves have been produced (11):

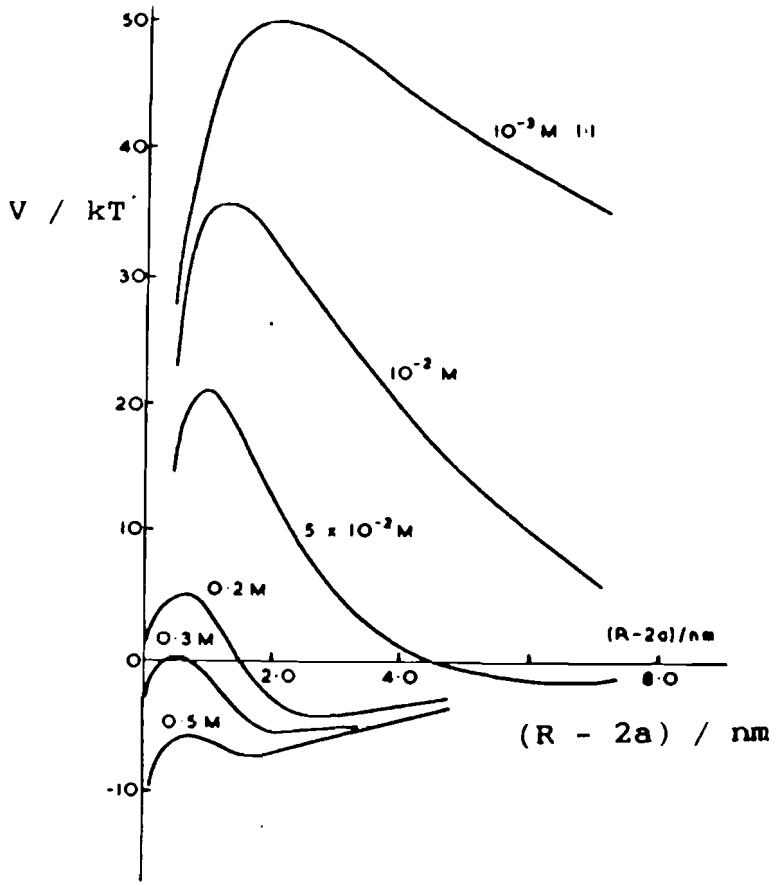

Here a loss of stabilisation may occur on addition of somewhere between 0.1 and 0.5 mol dm^{-3} 1:1 electrolyte. This is due to the fact that increasing the ionic concentration decreases the thickness of the electric double layer (ions of greater valency will have a greater effect), and this will reduce the height of the repulsive force barrier allowing particles to flocculate.

Figure 8. Effect of Particle Size

For large particles (1μm diameter) at moderate electrolyte concentrations, a secondary minimum may appear in the potential curve at longer distances of separation. Thus with large particles there is the possibility of weak reversible aggregation in the secondary minimum in addition to the strong contact aggregation which occurs in the primary minimum. This weak aggregation is sometimes referred to as flocculation so as to differentiate it from aggregation or coagulation (11).

PE DIGRAM FOR LARGE PARTICLE SIZE AND MODERATE IONIC STRENGTH ILLUSTRATING PRESENCE OF A SECONDARY MINIMUM

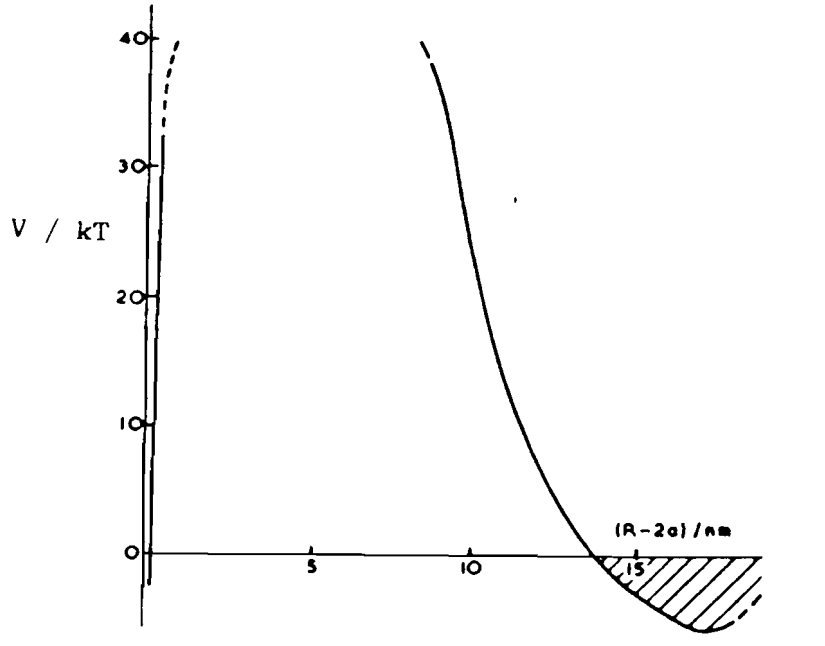

(R - 2a) / nm

4.3. SHEAR INDUCED AGGREGATION

Smoluchowski was the first to consider ortho-kinetic (shear induced) aggregation of colloidal particles (14). By neglecting interparticle forces and assuming that particles approach each other along rectilinear paths, he predicted that the collision frequency would be:

$$\frac{4 N \phi \dot{\bar{Y}}}{\pi} = \frac{16}{3} N^2 a^3 \dot{\gamma} \qquad \ldots\ldots (24)$$

where N = No. particles / unit volume
ϕ = volume fraction
$\dot{\bar{Y}}$ = shear rate
a = particle radius

This equation would give the rate of shear induced aggregation if each collision were successful.

Goren (6) investigated the effect of hydrodynamic forces on shear induced aggregation. He found that in general, the hydrodynamic forces exerted by a doublet of touching spheres in a shear flow, must be greater than the electrostatic stabilising forces between the spheres for aggregation to occur. A typical interparticle force diagram is shown below:

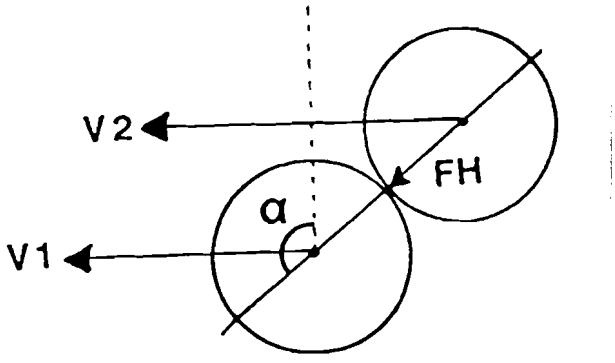

Figure 9.

Hydrodynamic forces between touching spheres in a shear flow.

For equal sized spheres of radius 'a' in a shear flow , the hydrodynamic force F_H acting along a line between the centres of the spheres is given by:

$$F_H(\alpha) = 6\,\pi\,\eta\,a^2\,\dot{\gamma}\,f\cos\alpha \times \cos(90-\alpha) \quad \ldots\ldots\ldots (25)$$

where η = shear viscosity
f = a tabulated function depending upon the ratio of the particle radii (2.04 for equal sized spheres)

As one particle approaches the other, α lies between 90° and 180° and F_H is negative (i.e. attractive). The maximum force pushing the particles together occurs for $\alpha = 135°$.

$$\left|F_H(\max)\right| = 6 \times 1.02 \times \pi\,\dot{\gamma}\,a^2\,\eta \times 10^{12} \quad \text{pN} \quad \ldots\ldots (26)$$

for equal sized spheres

The propensity for shear induced aggregation will therefore depend upon the balance of shear and DLVO forces. In particular comparison must be made between the repulsive force barrier and the maximum shear force available at the relevant shear rate.

i.e. No. of collisions x f [F_T, F_H (max)]

Previous work carried out by Zeichner and Schowalter (15) using trajectory analysis has produced results which can be summarised by the following stability domain diagram:

Figure 10. Balance of Hydrodynamic and Colloid Forces

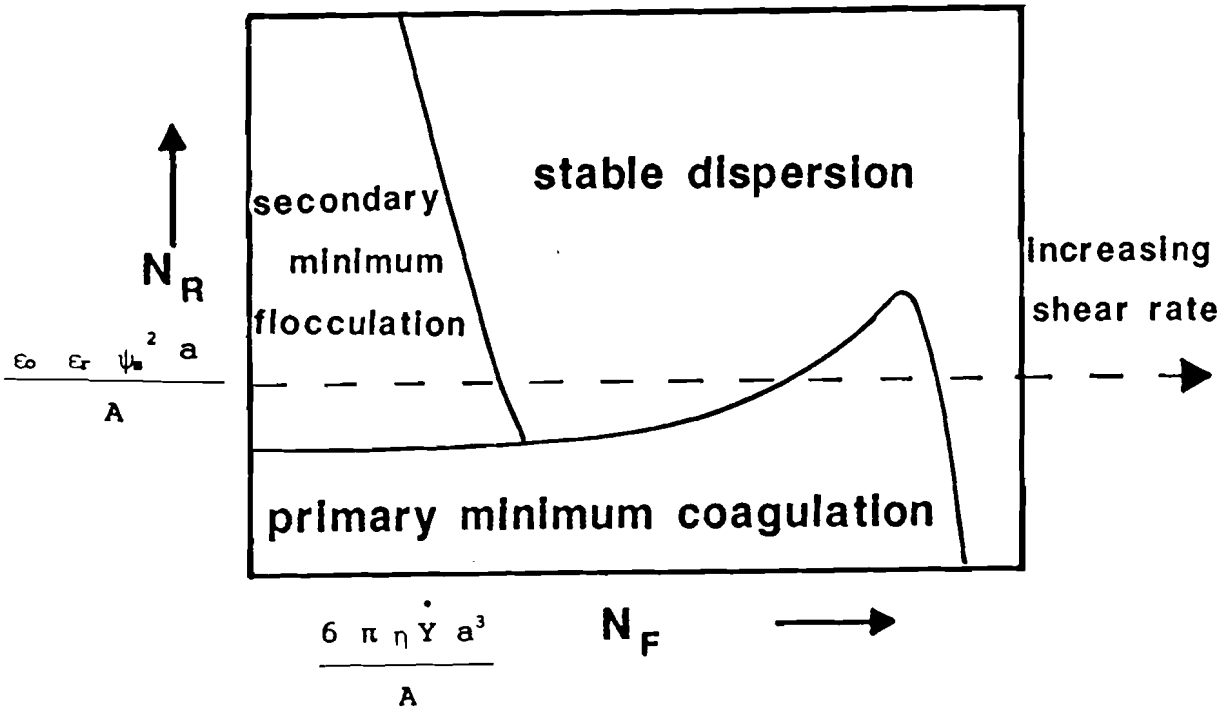

At rest the latex may be either dispersed, flocculated in the secondary minimum or aggregated depending upon the ionic strength. At low shear rates the weak flocs will break down into single particles. Applying an increasing shear rate will cause dispersion from the secondary minimum followed by coagulation into the primary minimum. A further increase in shear rate may lead to break up of the aggregates.

5. Characterisation of Lytron 2503

5.1. Infra Red Analysis

A sample of Lytron 2503 was scanned using a Perkin Elmer 680 Infra Red Spectrometer, to confirm that the latex was polystyrene.

A zinc selenium disc was used to mount the dried latex sample. Zinc selenium is preferable to the usual KCl or KBr discs in that they can be easily handled and washed under the tap after use. ZnSe absorbs IR radiation at wavenumbers < 600 cm^{-1}.

Result

The resulting trace is attached as Figure 11. The main peaks have been assigned and are summarised in Table 1.

Discussion

The Lytron 2503 trace compares very well with the reference polystyrene trace (Figure 12) and the absorbance peaks are consistent with those expected for polystyrene (16).

Table 1

INFRA RED CHARACTERISTICS OF LYTRON 2503

ABSORBANCE PEAK (WAVENUMBER cm^{-1})	POSSIBLE CAUSE
3100 - 3000	SEVERAL SMALL BANDS DUE TO AROMATIC C-H STRETCHING
2850, 2920	ALIPHATIC C-H STRETCHING
1600	AROMATIC C-C STRETCHING
1490	AROMATIC C-C STRETCHING
1460	$-CH_3$ AND $-CH_2-$ BENDING
1200 - 800	FINGERPRINT REGION. MANY SMALL PEAKS CHARACTERISTIC OF A SPECIFIC COMPOUND
760	OUT OF PLANE BENDING OF 5 ADJACENT H 'S ON AROMATIC RINGS
700	RING BENDING

5.2. Electronmicroscopy

Electronmicroscopy has been used extensively to measure the particle size and assess the dispersity of colloidal particles (7).

In this study the polystyrene was viewed in the scanning electron microscope. In the microscope a beam of electrons is accelerated towards the anode via the specimen. At some points along the path, the electron beam is deflected by fields controlled by the 'scan generator'. As a result the beam is moved over the specimen surface in a predetermined form such as a television raster. These primary electrons produce secondary electrons at the specimen surface and are detected by an electron collector. An image of the specimen is obtained which has good depth of field and reasonable resolution.

Micrographs of a few arbitary regions of the sample were collected. A visual assessment of these micrographs gave a qualitative measure of the degree of polydispersity of the polystyrene spheres.

Experimental

The latex was diluted to a low concentration (approx.10^{-3} g dm^{-3}) with distilled water. An air brush was used to spray the dilute samples onto freshly cleaved mica surfaces. The conductivity of the mica sheets was improved by sealing the edges to the metal stub using nickel paint and by gold coating the samples.

Results

Plates 3 and 4 indicate that the polystyrene is fairly monodisperse There are however a few very small particles which have been ignored for the purposes of this study.

Surface Characterisation

5.3. 1. Cleaning by Serum Replacement

Monodisperse polystyrene latices have been used extensively as model colloids for research and development as well as for industrial applications. An essential condition for their use is that the surface must be well characterised and the aqueous phase must be free of solute electrolyte and emulsifier. This condition can be achieved by a two step process of cleaning and surface characterisation. Previously latices have been cleaned by methods such as ion exchange or dialysis (17,18). However these techniques have limitations. Ion exchange is a rapid process which gives qualitative results, but requires purification of the ion exchange resin to remove the leachable polyelectrolytes which could absorb onto the latex particles. Dialysis is a slow process which in many cases only removes part of the emulsifier. Vanderhoff et al (19) described a new serum method in 1979 which is simple, quick and gives results in good agreement with ion exchange without arduous purification of the resin. Type 1 water (conductivity < 0.1 uS) is pumped through the latex while the particles are confined in a stirred cell by a filtration membrane of controlled pore size. This washing removes the solute electrolyte and adsorbed emulsifier. Further washing with dilute HCl followed by H_2O to remove excess acid replaces the Na^+ and K^+ counterions with H^+ ions.

If the protonated latex is now titrated with NaOH and the pH and the conductance of the system measured, the surface charge density of the sulphate and carboxyl surface groups can be calculated.

During the titration of the protonated latex with the NaOH, the conductance of the suspension drops initially as the more conductive hydrogen ions are neutralised with hydroxide and replaced by Na^+ ions. When all of the H^+ ions are neutralised, further addition of NaOH contributes free OH^- ions to the solution and the conductance rises again.

Experimental Serum Replacement

The filtration cell used for serum replacement is outlined in Figure 13.
Approximately 20 g of the latex was diluted to 80 cm^{-3} with deionised water and placed into the cell. An Amicon filtration membrane with a molecular weight cut off of 50,000 was supported by a porous polyethylene disc at the bottom of the cell. A Teflon coated stirring bar rotated close to the membrane surface to prevent clogging of the membrane and to give a steady flow rate over long periods of time. Water was fed from a reservoir into the top of the cell under a slight pressure to replace the serum by flushing it through the membrane. The filtrate was collected and its conductivity measured at regular intervals. This process was continued until the conductance of the filtrate fell to about the same level as that of the water feed.

Figure 13. Serum Replacement

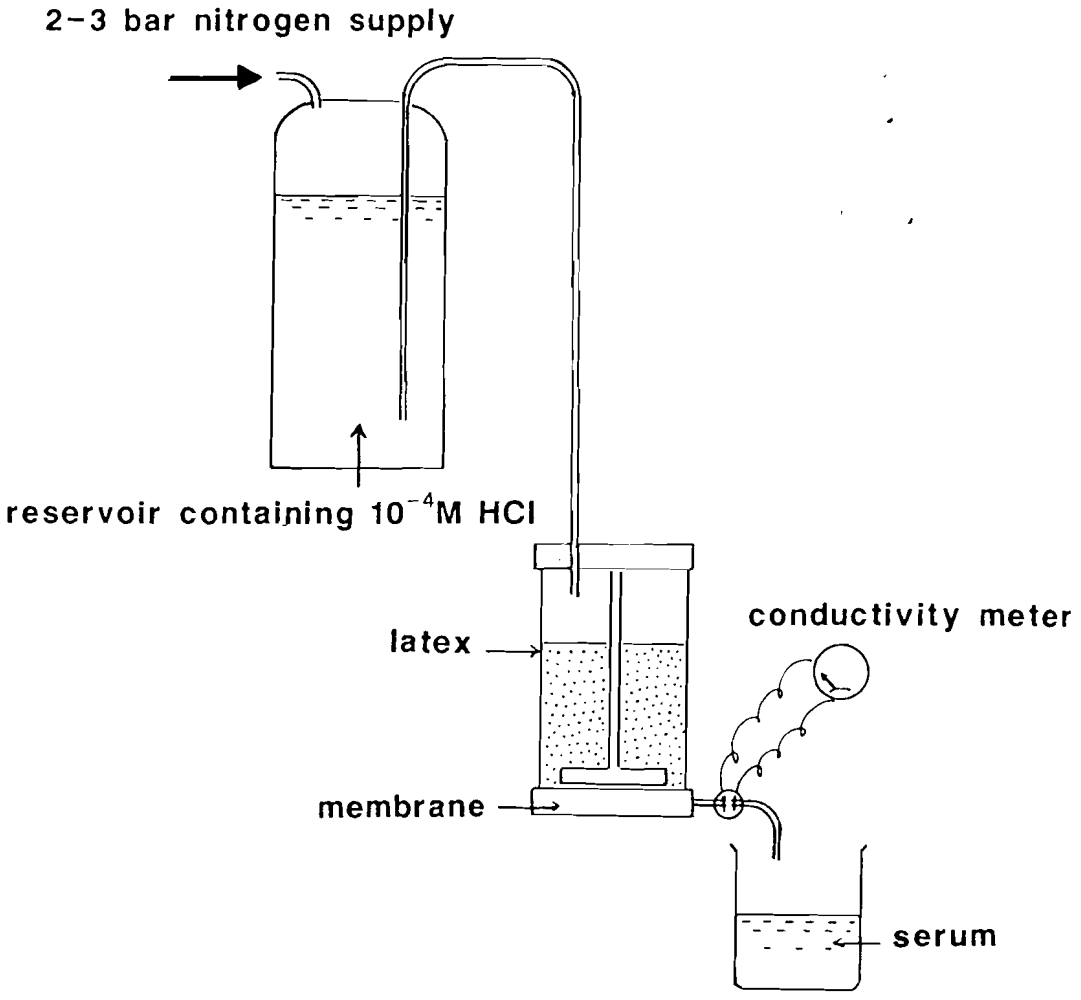

Results - Serum Replacement

The conductivity of the filtrate passing through the diafiltration cell was monitored with respect to the volume of filtrate collected. A graph of log conductivity against volume of filtrate collected is attached as Figure 14 . The diafiltration of the Lytron 2503 with dilute acid was continued until the conductivity was approximately the same as that of the washing solution. Approximately 2 litres of filtrate had to be collected for 20 g of latex to be cleaned and the surface acid groups protonated.

It was observed (Figure 14) that the conductivity of the filtrate fell initially to a lower value than that of the wash water. This is probably due to the ion exchange taking place between the Na^+ and K^+ counter ions on the latex surface and the H^+ ions from the acid. When the ion exchange was complete and the latex was fully protonated the conductivity of the filtrate rose to that of the dilute acid washing solution.

Figure 14

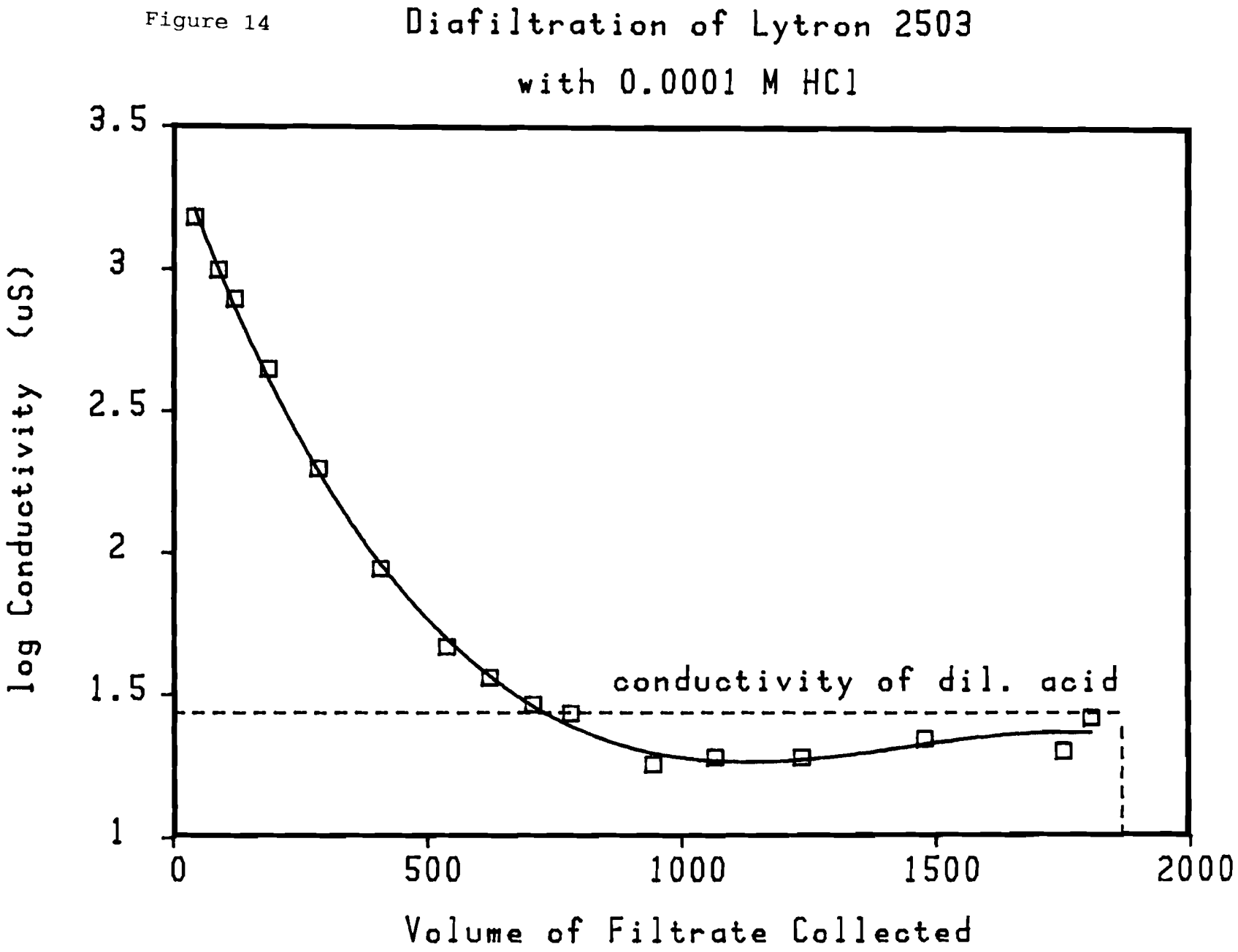
Diafiltration of Lytron 2503
with 0.0001 M HCl
log Conductivity (uS)
3.5
3
2.5
2
1.5
1
conductivity of dil. acid
0
500
1000
1500
2000
Volume of Filtrate Collected

5.4. Surface Charge Determination By Conductometric and Potentiometric Titration

Experimental

The apparatus was assembled as shown in the diagram below (Figure 15). The solutions were thermostatted to 25°C in a water bath prior to use. 1g (dry weight) of cleaned protonated latex was diluted to approximately 200 cm^3 with type 1 water (conductivity < 0.1 us) and transferred to a beaker.

The latex suspension was titrated with 0.01 M NaOH solution and the pH and conductivity changes noted.

Figure 15. Apparatus for Surface Charge Determination by Titration

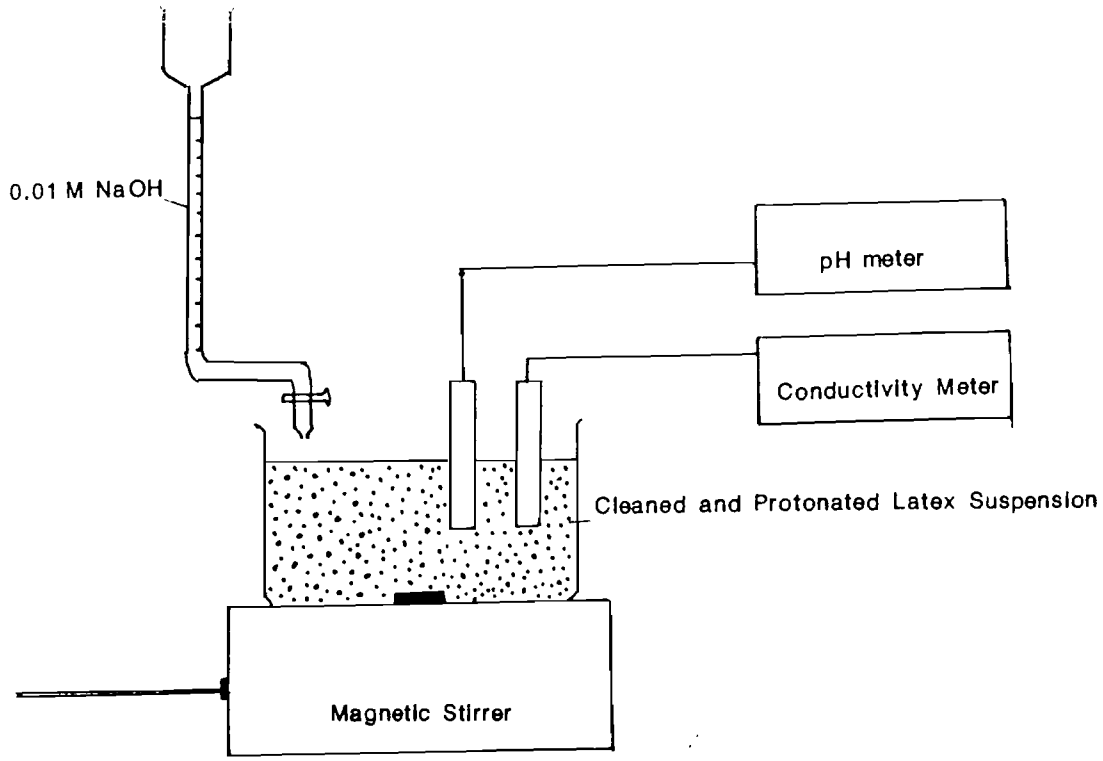

Results Surface Charge Determination

The conductometric and potentiometric titration results are illustrated in Figure 16. The conductivity results exhibit 2 inflection points; the first after the addition of 0.55 mls of 0.01M NaOH at pH 5, this corresponds to the strong acid sulphate groups, the second occured after the addition of 1.60 mls. of 0.01 M NaOH at pH 8 and corresponds to the weak acid groups.

The surface charge due to the sulphate and carboxyl groups on the cleaned protonated latex have been calculated as follows :

End points determined by potentiometric and conductometric titrations.
End points (1) strong acid $-SO_4^-$ groups = 0.55 mls NaOH
(2) weak acid $-COO^-$ groups = 1.60 - 0.55 = 1.05mls

(1) Strong acid group determination

$$(0.55/1000) \times 0.01 = 5.5 \times 10^{-6} \text{ mol NaOH}$$

1 mole of NaOH contains 6×10^{23} Na^+ atoms
Thus the number of Na^+ groups in the 1.0g of Lytron 2503 used

$$= (5.5 \times 10^{-6}/1) \times 6 \times 10^{23} = 3.3 \times 10^{18} \text{ } Na^+ \text{ atoms}$$

Each Na^+ atom requires 1 electron to neutralise it.
Charge on 1 electron = 1.602×10^{-19} coulombs

$$\text{Therefore } SO_4^- \text{ charge} = 1.602 \times 10^{-19} \times 3.3 \times 10^{18}$$

$$= 0.529 \text{ coulombs } g^{-1}$$

The surface area of a sphere = $4 \pi r^2$

Lytron 2503 has a radius = 0.241μm

Surface area = $4 \times 3.142 \times (0.241)^2 = 0.730 \ \mu m^2$

$$= 0.730 \times (10^{-6} m)^2$$

$$= 0.730 \times 10^{-12} \ m^2$$

Volume of a sphere = $4/3 \times \pi r^3$

$= 4/3 \times 3.142 \times (0.241 \times 10^{-6})^3$

$= 5.863 \times 10^{-20}\ m^3$

Volume of 1 particle = $5.863 \times 10^{-20}\ m^3$

Latex density = 1.05 gcm^{-3} = $1.05 \times 10^6\ gm^{-3}$

Weight of 1 particle = volume x density

$= 5.863 \times 10^{-20} \times 1.05 \times 10^6 = 6.156 \times 10^{-14}$ g

Specific surface area = $(0.730 \times 10^{-12}/6.156 \times 10^{-14})\ m^2g^{-1}$

$= 11.858\ m^2g^{-1}$

From titration results surface charge on particles = 0.529 C g^{-1}

Therefore surface charge from SO_4^- groups

$= (0.529/11.858) = 0.0446\ C\ m^{-2}$

$= 0.0446 \times 10^6\ \mu C\ m^{-2}$

$= 4.46 \times 10^4\ \mu C\ m^{-2}$

For $\mu C\ cm^{-2}$ multiply by 10^{-4}

= 4.46 $\mu C\ cm^{-2}$ from sulphate groups

(2) Weak acid group charge determination

1.05 mls 0.01 M NaOH needed for end point

$(1.05/1000) \times 0.01 = 1.05 \times 10^{-5}$ mol NaOH

1 mol contains 6×10^{23} Na^+ atoms

$(1.05 \times 10^{-5}/1) \times 6 \times 10^{23} = 6.3 \times 10^{18}$ Na^+

atoms in 1g Lytron 2503

Each Na^+ atom needs 1 electron to neutralise it.

Charge on 1 electron = 1.602×10^{-19} coulombs

Therefore the charge on the surface due to the $-COO^-$ groups

$= 6.3 \times 10^{18} \times 1.602 \times 10^{-19}$

$= 1.009$ C g^{-1}

As calculated previously specific surface area = 11.858 m^2 g^{-1} for Lytron 2503.

Therefore the surface charge from the COO^- groups

$= (1.009/11.86) = 0.08508$ C m^{-2}

$= 0.08508 \times 10^6$ µC m^2

For µC cm^{-2} multiply by 10^{-4}

= 8.5 µC cm^{-2} from carboxyl groups

Surface charge Determination

Discussion

The surface charge values calculated for the sulphate surface groups are comparable to those found in previous studies (Vanderhoff et al (19) determined 1-5 $\mu C\ cm^{-2}$ for polystyrene latices). Discussion with Prof. R H Ottwill (University of Bristol) has confirmed that a value of 4.5 $\mu C\ cm^{-2}$ for surface sulphate groups on a model polystyrene latex is a typical value. However the value for carboxyl surface charge groups was considered to be higher than expected for a pure polystyrene latex in which the carboxyl groups are produced by a side reaction during manufacture.

However Lytron 2503 is a polystyrene latex which is used in paper coating applications and as such has probably been manufactured using a deliberate polyacrylate addition (10) which results in a higher degree of carboxylation than normally encountered in a model colloid. Carboxyl groups have a beneficial effect in paper coating latices, as they help bind the latex onto the pigment particles.

Figure 16

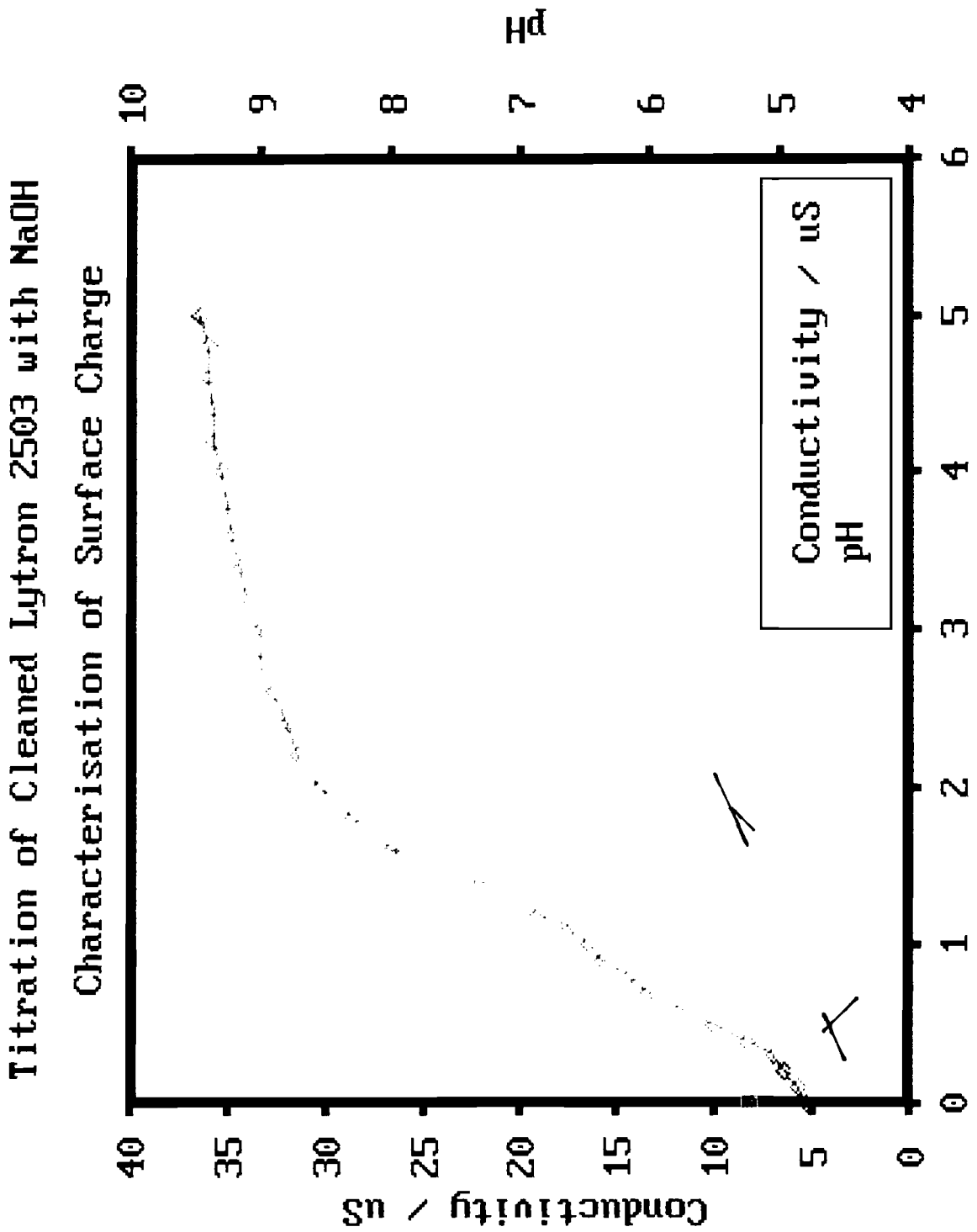
Titration of Cleaned Lytron 2503 with NaOH
Characterisation of Surface Charge
Conductivity / uS
pH
Volume 0.01 M NaOH added
Conductivity / uS
pH
0
5
10
15
20
25
30
35
40
4
5
6
7
8
9
10
0
1
2
3
4
5
6

6.1. VISCOSITY / SHEAR RATE THEORY

The viscosity and rheological behaviour of a liquid can best be described by considering a cube of fluid with length "L" as shown below:

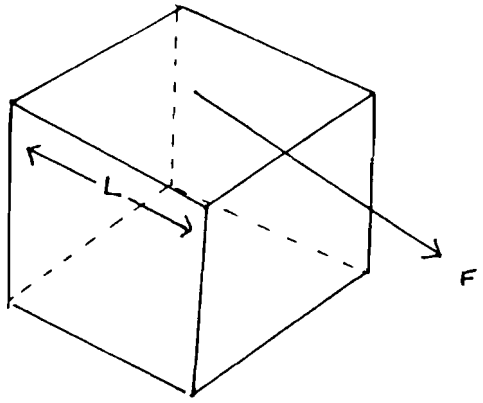

If the liquid cube is pulled in tension it would continue to extend as long as the force were applied and would not recover when the force was removed. This behaviour is indicative of flow. If one face of the cube was fixed and then a force "F" was applied tangentially over the opposite face then the cube distorts so that the two opposite faces become parallelograms. This is known as simple shear and is often described by the shear angle θ (20).

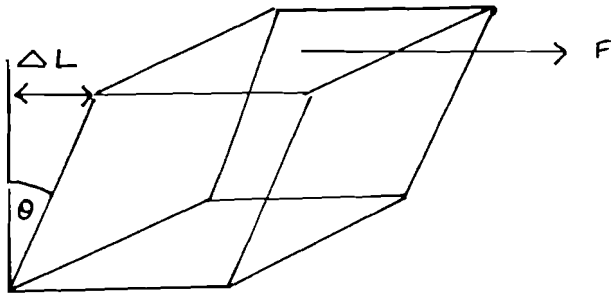

In a liquid however, as the cube 'distorts' in the direction of the force, liquid will move in from the left to fill up the gap. The movement is continuous as long as the force is applied and the angle of shear changes continually. The rate of shear is now measured and is equal to $\delta\theta/\delta t$ with units of reciprocal seconds. As the liquid molecules are moved over one another in the shearing action, intermolecular forces of attraction between the molecules gives rise to some resistance. This force of resistance is known as viscosity. Viscosity is defined by Newton's Law, as the ratio of shear stress to shear rate for any fluid,

i.e. $\eta = \tau / D \quad \therefore \quad \tau = \eta D \quad \ldots\ldots (27)$

where τ = shear stress η = viscosity D = shear rate

Viscosity has the units of mPa.S (milli pascal seconds).

In the special case where n is a constant independant of shear rate, the fluid is said to be "Newtonian", for example a plot of shear rate vs. shear stress for a simple liquid such as water or an oil, is a straight line through the origen.

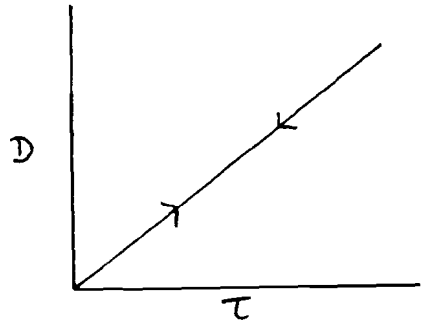

However many materials including suspensions of latex particles exhibit non Newtonian behaviour. Latex suspensions are usually shear thinning, i.e. the viscosity decreases with increasing shear. This behaviour can be described by considering a suspension of particles connected by extensible 'links', which stretch and break off. With increasing shear rate these links progressively detach and with decreasing shear rate they re-attach. The flow curve may look as follows:

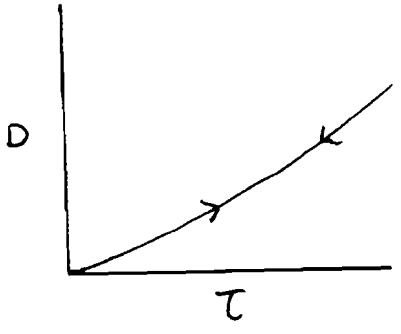

Bohlin VOR Rheometry - Experimental Section

The Bohlin VOR (viscosity - oscillation - relaxation) is a modern controlled strain rate rheometer which is capable of making a large variety of rheological measurements. It incorporates a wide selection of geometries which can be used to measure the viscosity at a wide range of shear rates (10^{-3} s^{-1} - 10^{5} s^{-1}); laminar flow is expected up to the very highest shear rates. A number of torque bars are also available allowing the maximum sensitivity to be achieved for each geometry and sample system. The torque bars range from 30uNM to 30mNM and sensitivity down to 0.1% of the full scale deflection can be achieved.

The rheometer is interfaced to a computer which is equipped with 'user friendly' software packages as well as data processing and output options. Photographs of the instrument are included as Plates 5 and 6.

An outline of the principle parts of the rheometer is shown below in Figure 17:

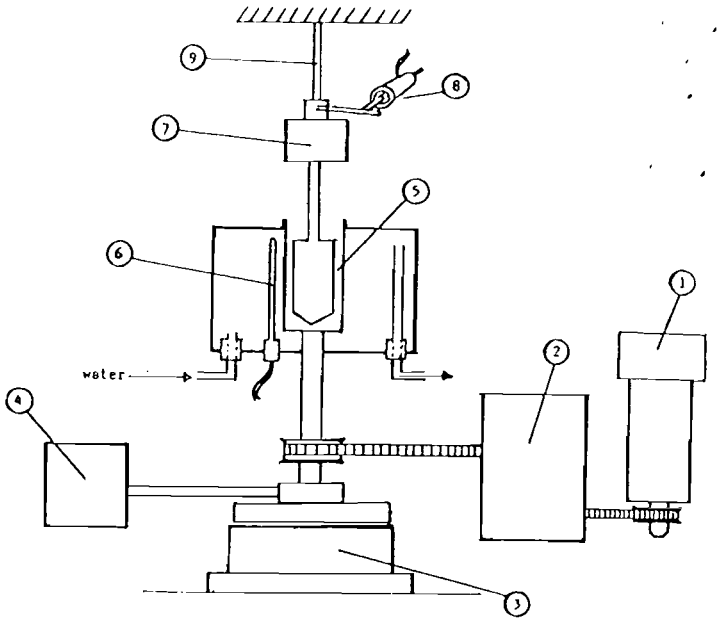

1 - DC motor with tacho servo
2 - Gear boxes
3 - Clutch
4 - Position servo actuator
5 - Sample cell
6 - Temperature sensor
7 - Air bearing
8 - LVDT torque measurement
9 - Torque bar

Figure 17. Principle parts of a Bohlin VOR Rheometer

The three essential parts of this rheometer are the dc motor, the measuring head (tapered plug with cup) and the torque measurement system.

The outer cup is rotated (producing a shear rate or shear strain) and the viscous resistance generated is measured by the torque system. This torque value is converted into a value of shear stress (expressed as force/unit area, Pa). Motor speed, measuring head geometry and gap size determine the shear rate applied. Knowing the shear rate and the shear stress, the viscosity can be calculated using equation 27.

To obtain the high shear rates necessary to model the behaviour which occurs on a commercial paper coating machine, the tapered plug attachment was used. The tapered plug measuring geometry allows shear rates of up to 10^5 s^{-1} to be obtained. The shear rate can be altered by either adjusting the speed of the rotation or the size of the gap.
This geometry is outlined below:

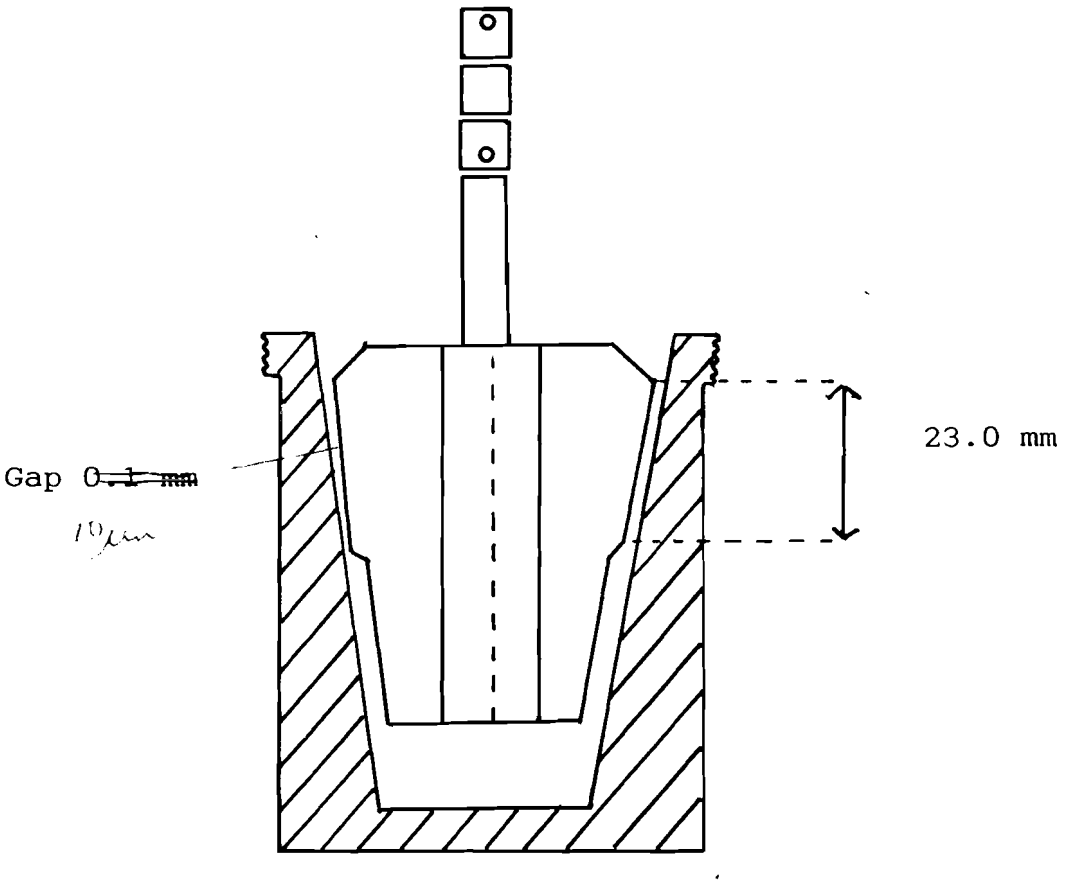

Figure 18. Tapered plug measuring geometry
The latex samples were diluted to 10% solids for all rheological measurements. The gap was set to 0.1 mm and the samples were inserted carefully with the cup rotating slowly (~100 s^{-1}).

The Bohlin Rheometer was used for two functions:

1) To produce a shear rate / shear stress / viscosity set of curves for each sample. These shear rate and viscosity values were inserted into Gorens' equation to calculate the hydrodynamic forces produced during shearing.

2) As a shearing device to shear the samples at a single predetermined shear rate for a fixed time.

6.2. DYNAMIC LIGHT SCATTERING - PHOTON CORRELATION SPECTROSCOPY

In conventional light scattering, the light scattered from a suspension of particles is of random phase so that destructive interference does not occur in a systematic way. If however a laser is used the light is coherent (i.e. the wave motion is in phase across a plane of propagating light) and interference patterns are produced by an array of particles. If the particles are stationary, a diffraction pattern of bright spots can be seen. In a colloidal dispersion particles are in continuous motion and a mobile 'speckle pattern' results. Dynamic Light Scattering is a technique which enables the correlation in time between the fluctuations in light intensity to be analysed (21).

In Photon Correlation Spectroscopy (PCS) laser light of coherent wavelength (λ = 6328 Å) is shone through a dilute colloidal dispersion (22). During the passage of a photon through the suspension there exists a small finite probability that it will encounter a particle and be scattered. The energy change imparted by the motion of the particle is indicated by a small change in frequency of the scattered radiation. The amount that the photon is scattered or deflected is measured by the intensity at the scattering angle 2θ, and is dependent upon the size and shape of the particle. A photomultiplier tube (PMT) allows the number of photons arriving at a given scattering angle in a given time to be monitored.

Suppose at time "t" the number of photons arriving at the PMT in a time interval $\Delta\tau$ for a given scattering angle "2θ", is given by n(t). The time interval $\Delta\tau$ is considered to be of the order of microseconds. A plot of n(t) against t can be illustrated as follows:

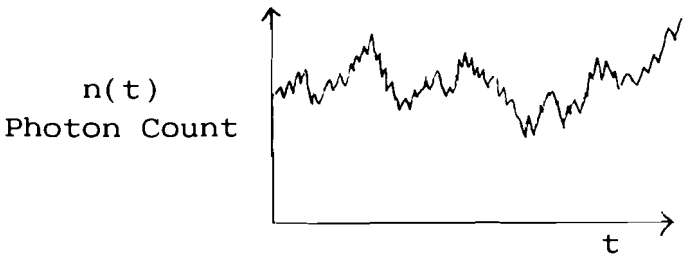

Figure 19. The number of photons arriving at PMT in time t.

At first glance such a plot could be considered random white noise. However particles of a given size in a fluid medium undergo translational diffusion D_T (m^2s^{-1}) due to the effects of

Brownian motion imparted by bombardment of solvent molecules of thermal energy kT. As they move through the liquid the particles experience a resistance equivalent to viscous drag:

$$6 \pi \eta (a/2) \qquad \ldots\ldots (28)$$

where η = viscosity of medium
a = equivalent spherical diameter

The ratio of these 2 quantities (Brownian motion : viscous drag) determines the rate of diffusion:

$$D_T = \frac{kT}{3 \pi \eta a} \qquad \text{where k = Boltzmann constant} \qquad \ldots\ldots (29)$$

Thus the photon count signal in Figure 19 contains information in the frequency domain about the rate of particle diffusion. To obtain a 'lifetime' at which a particle remains in the scattering position, known as the correlation time τ_c, the following calculations are made.

A replica of the information in Figure 19 is collected by the computer after a time delay $\Delta\tau$ and is superimposed over the original. The area of the product of the functions is recorded. The time delay is then incremented and the procedure repeated until the experiment duration t is exhausted.

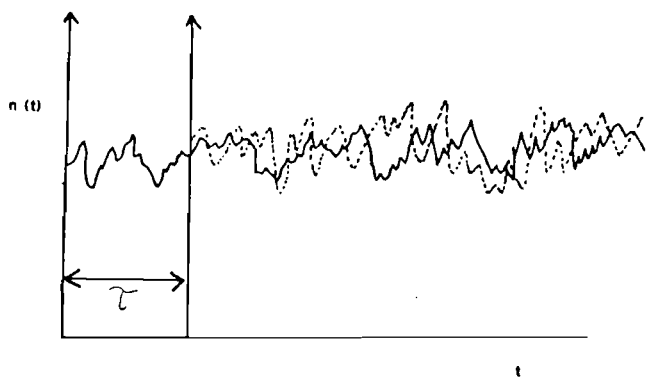

Figure 20. Number of photons at PMT after a time delay

This process measures the rate of decay of correlation within the signal n(t) i.e. its autocorrelation c(τ). In the idealised case of monosize spherical particles the functional form of c(τ) is a single exponential decay characterised by

$$c(\tau) \quad e^{-\tau/\tau_c} \quad < n(t)\ n(t+\tau) > \qquad \ldots\ldots (30)$$

where τc is the correlation time and n is the refractive index of the medium. The correlation time τc is related to the diffusion coefficient by

$$1/\tau c = D_T\ q^2 \qquad \ldots\ldots (31)$$

where q the scattering vector is given by

$$|\underset{\sim}{q}| = \frac{4\ \pi\ \eta}{\lambda}\ \sin\ \theta \qquad \ldots\ldots (32)$$

Hence a measure of τc can result in a measure of the equivalent spherical diameter (a) of the particles via the Stokes Einstein equation (29).

PCS is now widely used for the determination of the size of particles in the colloid range. In general the results are in good agreement with those found by electron microscopy. Discrepancies which may occur may be attributed either to a difference between the hydrodynamic radius (which includes any solvent sheath or adsorbed layer on the surface of the particles, this is measured by the PCS) and the real radius, or to changes in the particle size arising from the preparation (drying) of the sample for electron microscopy or arising from the bombardment by the electron beam. For polydisperse systems or those systems with non spherical particles the results are less accurate, and interpretation of the data more complex.

Experimental Section PCS

The Malvern K7025 Photon Correlation System was used to measure the particle size of the polystyrene spheres by laser light scattering. The major components of the apparatus are illustrated below:

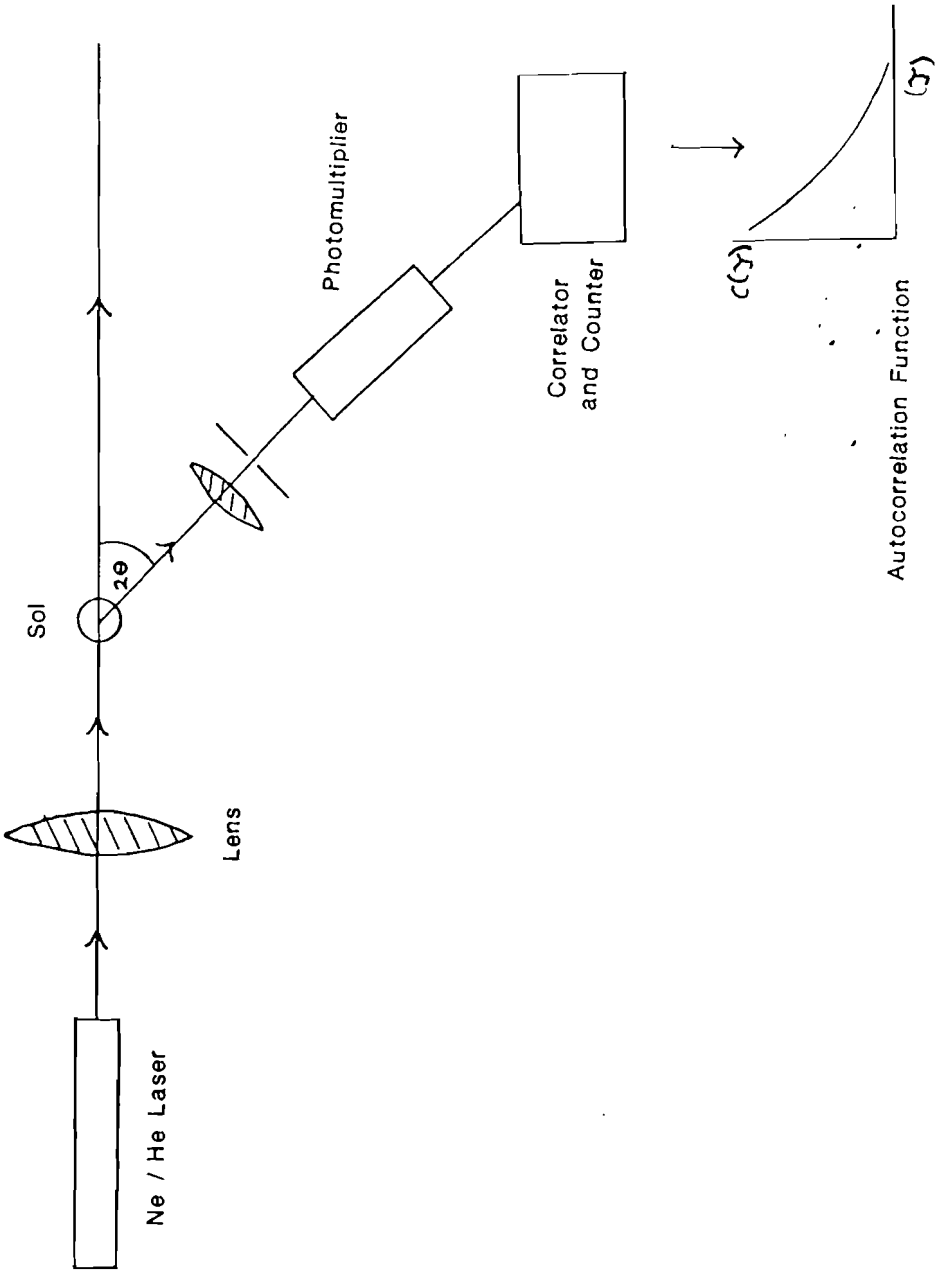

Figure 21. An outline of the components in the Malvern K7025 Photon Correlation System

The latex samples were diluted with distilled water to a concentration of approximately 1 . 10^{-4} gdm^{-3}. A portion of the sample to be measured was transferred to a clean glass cell which was placed in a controlled temperature water bath (25°C). (**NB** the liquid in the bath must have a refractive index which matches that of the diluting medium).

The laser light was of wavelength 6328 A and the PMT was positioned at a scattering angle (2θ) of 90° for all the measurements. 10 particle size measurements were taken for each sample and the results were averaged.

6.3. Electrophoresis Measurements for Zeta Potential Calculation

The magnitude of the repulsive forces between particles is dependent upon the electrical charge density of the shear plane (σ) of the particle. This value is closely related to the zeta potential which can be calculated by measuring the electrophoretic mobility (u) of the colloidal system. Particle electrophoresis experiments give a method of measuring the electrophoretic mobility (23).

Electrophoresis is an electrokinetic phenomenon. In general terms, it is the induced tangential movement of one phase past a secondary contacting phase by the application of an electric field. When one phase consists of a liquid or gas in which the second phase is suspended as particles, then electrophoresis is said to have occurred when the particles are induced to move relative to a stationary liquid by an applied electric field.

The derivation of the u/z and z/σ relationships beginning from the Poisson - Boltzmann equation is a straight forward procedure when the size of the colloid system particle of radius 'a' (out to the shear plane) is such that $ka >> 1$ or $ka << 1$.

k^{-1} is known as the Debye Huckel reciprocal length and represents the effective thickness of the electrical double layer. The potential of the double layer which decays exponentially with distance over the surface is extremely sensitive to the electrolyte concentration.

$$k = \left[\frac{2 \times 10^3 N e^2}{\epsilon_o D kT} \right]^{1/2} \times \left[\frac{1}{2} \sum_i c_i z_i^2 \right] \quad m^{-1} \qquad \ldots\ldots (33)$$

where N = Avogadros constant : 6.02×10^{23} mol^{-1}
e = Elementary charge : 1.60×10^{-12} $F\ m^{-1}$
ϵ_o = Permittivity of vacuum 8.85×10^{-12} $F\ m^{-1}$
D = Dielectric constant of continuous phase, taken to be water at 25°C = 78.36
k = Boltzmann constant : 1.38×10^{-23} JK^{-1}
T = Absolute temperature : 298.15 K

$$1/2 \sum_i C_i Z_i^2 = \text{Ionic strength (I)} \qquad \ldots\ldots (34)$$

C_i = Molar valency of ith species
Z_i = Valency of ith species (excluding sign)

Thus for a continuous phase of D = 78.36 @ 25°C

$$k = 3.29 \times 10^9 \, (I)^{1/2} \; m^{-1} \qquad \ldots\ldots (35)$$

For ionic concentrations of 10^{-3} m or greater and particle radii of 0.5 um the K_a values are large. This means that the particles can be considered large in comparison to the electrical double layer thickness which is regarded as a thin layer region around the particle surface. In this case the curvature of the particle surface can be ignored and the Poisson - Boltzmann equation (33) can be solved in planer geometry.

$$\psi = \left[\frac{4 \, KT}{Ze} \right] \exp (- \kappa H) \qquad \ldots\ldots (36)$$

The U/Z Relationship At Large k_a, Helmholtz - Smoluchowski Equation

In his paper (25) published in 1903 Smoluchowski derived a formula for u of a particle of arbitary shape. Smoluchowski's derivation was as follows :
If the particle is a non-conductor of electricity then the applied field has only 1 component parallel to the surface. As previously stated the particle surface can be considered as essentially flat with the motion of liquid in the adjacent diffuse part of the electrical double layer being parallel to the particle surface. The liquid in the double layer is therefore subjected to 2 forces of opposite directions, both parallel to the particle surface, one due to the applied electric field working on the surface charge and the other due to viscous friction. The volume element of liquid will rapidly attain a uniform velocity parallel to the surface, with the electrical and viscous forces balanced.

By equating these forces, inserting Poisson's equation and assuming relative permativity and viscosity, Smoluchowski obtained:

$$z = \frac{u\,\eta}{\epsilon_o\, D} \qquad V \qquad \ldots\ldots (37)$$

where η = absolute viscosity of continuous phase taken to be water @ 25°C : 0.8903×10^{-3} Kg M^{-1} S^{-1}

Thus for a continuous phase of D = 78.36 and
n = 0.8903×10^{-3} Kg m^{-1} s^{-1} we have

$$z = 1.283 \times 10^{-9} \times u \qquad mV \qquad \ldots\ldots (38)$$

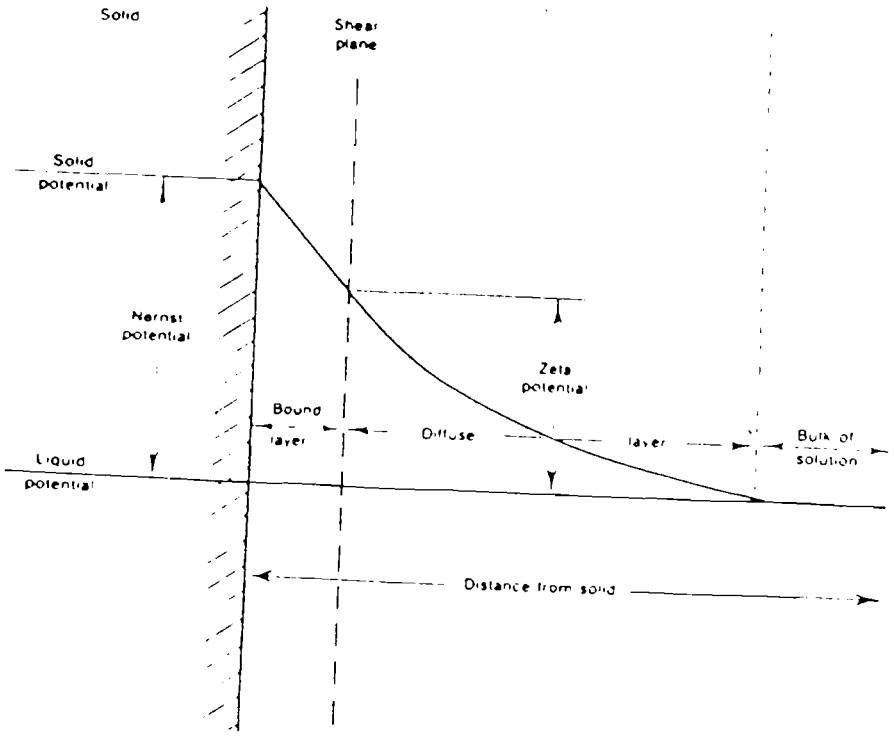

Figure 22. Diagam illustrating the zeta potential.

Electrophoresis Apparatus.

The electrophoresis apparatus was supplied by Rank Brothers. The instrument model was the Mk 2, which was fitted with a video camera and a television monitor.

The reversible metal electrodes were cleaned and platinised by electrodeposition using a solution of K_2PtCl_6 and lead acetate in 0.025M HCl.

Several calibrations were necessary prior to making the electrophoretic measurements. Firstly, the thickness of the glass cell was measured by focusing on the back and front inside surfaces of the cell. The apparent thickness in water at 25°C (refractive index = 1.333) was typically ca. 0.75mm, i.e. real thickness typically ca. 1.00mm. The height of the cell was measured using a travelling microscope. The "real" height was 10.0mm, giving a real cross-sectional area of $10.0mm^2$. The effective distance between the electrodes was calculated by measuring the resistance (R) of a solution of 0.1M KCl. The solution was placed in the cell, the electrodes were inserted and the cell was thermostatted at 25°C. The resistance was measured using a Universal bridge operating at a frequency of 1kHz. The effective distance was found to be exactly 7cm.
The observed horizontal length (f_g) in the cell that was equivalent to one division of the television monitor was found to be 0.1mm.

Particle electrophoresis measurements are complicated by the simultaneous occurrence of electro-osmosis. The internal surfaces of the glass cell are generally charged and the applied electric field causes not only electrophoretic migration but also an electro-osmotic flow of water close to the cell walls with a compensating return flow of water with a maximum velocity at the centre of the cell. Hence the true electrophoretic migration is only observed at two positions in the cell where the electro-osmotic flows are cancelled by the return flow, i.e. at zero velocity on the liquid velocity profile diagram shown in Figure 23 :

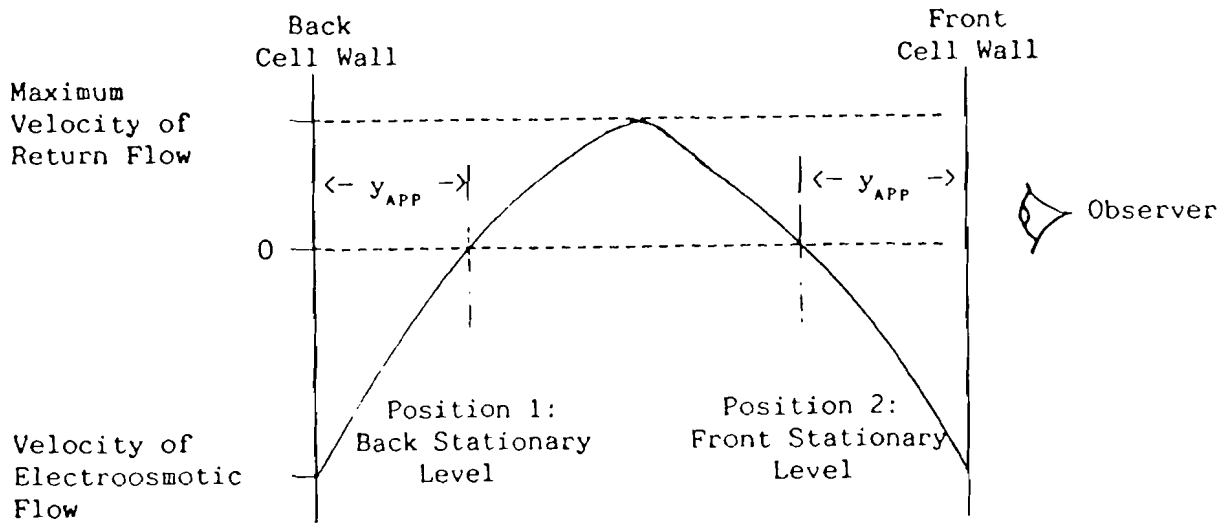

Figure 23. Liquid Velocity Profile Diagram

The "real" distance (y_{real}) from a cell wall to a stationary level is given by;

$$y_{real} = b - b\left[\frac{1}{3} + \frac{128b}{\pi^5 a}\right]^{1/2} \qquad \ldots\ldots (39)$$

where 2b = thickness of the cell (10.0 mm)
2a = height of the cell (1.00 mm)

Thus y_{real} = 0.19mm and the apparent distance (y_{app}) from a cell wall to a stationary level when viewed through water at 25°C is 0.15mm.

Serum removed from a 10% solution of latex by diafiltration was used to dilute small portions of the latex to 0.0025 wt.%. Using this serum ensured a background ionic strength similar to that of the latex used in the shearing experiments. The latex samples in 0.1, 0.01 and 0.001 M NaCl were diluted to 0.0025 wt.% using these standard salt solutions. Each dispersion was flushed through the cell several times to ensure that the eventual contents of the cell were devoid of air bubbles. The electrodes were rinsed with the dispersion prior to being inserted into the cell. The cell was thermostatted at 25°C during measurements. The cell was positioned within the electrophoresis apparatus such that the same side of the cell always faced the light source. The voltage across the platinum electrodes was switched on). The most

convenient voltage for these samples was found to be either 40V or 50V. The video camera was focused at the centre of the cell, a negative polarity was applied, and the clay particles in the suspension moved from the left of the cell to the right of the cell. The particle movement, under this particular configuration indicated that the particles had a negative charge. The camera was then focused on the front stationary level (0.15mm away from the inside surface of the front interior cell wall). The time for an observed particle to move across one division of the observation graticule was measured. The voltage polarity was then reversed and a different particle was observed and timed moving in the opposite direction. This procedure was repeated at least a further four times, giving five "t" values in each direction for a given voltage.

The electrophoretic velocity (v) was calculated from the means of the reciprocal timings. The electrophoretic mobility was evaluated from the particle velocities at the front and back stationary levels, i.e. v_{FSL} and v_{BSL}, where

$$u = d_c . \frac{(v_{FSL} + v_{BSL})}{2V} \qquad \ldots\ldots (40)$$

in which $d_c = 7.0 \times 10^{-2}$m and V = 40 or 50 volts.

The zeta potential (ζ) can be calculated from the electrophoretic mobility, using equation (38).

7.1. Experiment 1

Samples of Lytron 2503 as received were sheared for periods of 20 seconds at a number of different shear rates using the Bohlin VOR rheometer. The residues of each sample were washed off the tapered plug, care was taken to prevent the collection of unsheared latex, and the mean particle size was measured using the PCS.

A shear rate / viscosity curve was also obtained for the sample over a shear rate range of 10^3 to 10^5 $sec.^{-1}$.

The Lytron 2503 was then sheared at a single shear rate of 78300 s^{-1} for a period of longer time scales ranging from 20 seconds up to 10 minutes. The particle size of the residues was again determined using PCS.

Previous work by J.C Husband (within ECC laboratories) on acrylic latices has shown that significant aggregation occured after shearing them for periods of 1 to 2 seconds and that after shearing for periods of 20 seconds no further aggregation was detected. For this reason all further samples have been sheared for 20 second periods.

The theoretical repulsive force barrier height (V_{max}) was calculated using the DLVO calculations as described on page 15. Certain experimental parameters were necessary before these calculations could be made; these being the ionic strength of the solution and zeta potential of the colloidal particles.

The zeta potential of the samples were measured using the Rank Brothers apparatus, using the method described on page 46.

The ionic strength of the 10% latex suspension was determined using conductivity measurements. The assumption was made that the latex ionic charge was mainly due to the sulphate surface groups. The conductivity of a series of standard Na_2SO_4 solutions was measured and a calibration curve constructed (Figure 27.). From this curve the salt concentration of the latex was determined.

The DLVO calculations were incorporated into a computer program for ease of use. The hydrodynamic forces incurred by shearing were calculated using Gorens equation as described on page 21. The viscosity / shear rate plot data was used to calculate the hydrodynamic force at a range of shear rates.

7.2. Experiment 2

The addition of electrolyte is known to depress the repulsive forces between particles (as described on page 18). It was thought that additions of known amounts of 1:1 electrolyte to the cleaned latex might depress the repulsive force barrier (Vmax) enough for the shearing action to aggregate the latex.

The latex as received contains many adsorbed ionic groups on its surface and the latex serum will contain emulsifier and inorganic salts. It was decided that to obtain a latex with known amounts of electrolyte for the shearing experiments, the latex must first be "cleaned" by diafiltration to remove any residual salts and by products of manufacture. This process was carried out as described previously for the latex characterisation, and surface charge determination (pages 25 - 26).

Portions of the "cleaned" salt free latex were diluted with standard 1:1 electrolyte to produce the following samples:

Sample 1 10% Lytron 2503 in 0.001 M NaCl
Sample 2 10% Lytron 2503 in 0.01 M NaCl
Sample 3 10% Lytron 2503 in 0.1 M NaCl

These samples were sheared in the Bohlin VOR and the particle size of the residues determined. The theoretical critical shear rates for each were calculated using Goren's equation and the DVLO theory as previously described.

7.3. Experiment 3

It was decided that by increasing the viscosity of the latex suspension, the hydrodynamic forces incurred by the shearing action would be increased, owing to the viscosity term in Gorens equation (equation 26).

It was considered that increasing the hydrodynamic force would outweigh the repulsive force barrier and cause aggregation of the latex. Sodium carboxymethyl cellulose is commonly added to coating colours and acts as a flow modifier by increasing the viscosity of the aqueous phase. It helps retain water in the

colour and causes it to increase in viscosity. The general formula for sodium carboxymethyl cellulose with a degree of substitution = 1, is shown below:

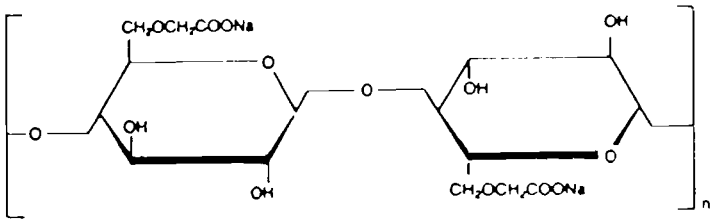

5% of a CMC called 7MID with an approximate molecular weight of 260,000 and a degree of substitution of 0.7 was added to the latex suspension. This mixture was sheared at a range of shear rates and the resultant particle size measured using PCS. A portion of the CMC / latex solution was diluted with latex serum to 0.0025 weight% for electrophoresis measurements.

The relative viscosity of the CMC / latex solution was required to calculate the electrophoretic mobility u. This was determined using an Oswald capillary viscometer as described below.

Relative Viscosity Determination

A clean Oswald viscometer (model D) was mounted vertically in a water bath which was thermostatted to 25°C. Deionised water was poured into the viscometer until the lower mark was reached. The water was sucked up to above the upper mark using a pipette filler. A stop-watch was started as the water flowed past the upper mark and stopped when it flowed past the lower mark in the viscometer. 10 readings were taken and the values averaged to give a viscosity related result for water. The experiment was repeated with the CMC / latex solution which had been diluted to 0.0025% with latex serum for the electrophoresis experiments.

The electrophoretic mobility was calculated as follows:

$$\frac{\text{averaged Oswald value CMC/latex}}{\text{averaged Oswald value water}} = \text{Relative viscosity}$$

$$Z = \frac{(\text{relative viscosity} \cdot \text{absolute viscosity} \cdot u)}{E_o \cdot D} \quad \text{volts}$$

The DLVO calculations were carried out as previously described and the hydrodynamic forces at each shear rate were calculated using Goren's equation.

8.1. Results - Experiment 1

The shear rate / viscosity curve produced for the Lytron 2503 sample as received is attached as Figure 24.
Figure 25 shows the mean particle size of the latex after shearing up to 124,000 s^{-1} for periods of 20 seconds. No aggregation of the latex was observed from these measurements.

The particle size measurements from the latex sheared at 78300 s^{-1} for longer periods of time is attached as Figure 26. No particle aggregation was attained after shearing the latex for up to 10 minutes.

The calibration curve obtained for the ionic strength determinations is attached as Figure 27 . A good straight line resulted when the log (conductivity) was plotted against the log (concentration) of a series of standard sodium sulphate solutions.

The DLVO potential energy and total force curves are included as Figure 28 . The repulsive barrier height (V max) was calculated to be 115 pN.

A graph showing the balance of hydrodynamic and DVLO forces is attached as Figure 29 . This graph predicts that the intercept of the DLVO repulsive barrier force with the hydrodynamic forces would occur at shear rates higher than those obtainable from the Bohlin Rheometer. It was therefore predicted that the latex would not aggregate at the shear rates used. This is in agreement with the experimental results.

A summary of the results is tabulated below:

Ionic strength = 0.011 M
Zeta potential = -42 mV

DLVO Force calculation V_{max} = 115 pN
DLVO Potential Energy kT_{max} = ~130 kT

Critical shear rate experimental = > 1.5×10^{-5} s^{-1} (not reached)
Critical shear rate theoretical = ~5.25×10^{-5} s^{-1}

8.2. Results - Experiment 2

Shearing experiments were not carried out on the cleaned latex before the electrolyte addition, because the low ionic strength greatly increases the effective thickness of the double layer. The particles can no longer be considered large in comparison with the e.d.l thickness and the zeta potential calculations as measured by the Helmholtz - Smoluchowski equation break down.

The shear rate / viscosity rheograms obtained for the three samples in standard electrolyte are attached as Figures 30, 31 and 32.

The calculated DLVO force and potential energy distance curves are attached as Figures 33 and 34. It can be seen from these that the addition of salt characteristically decreased the thickness of the electric double layer around the latex particle. The Lytron 2503 in 0.1 M NaCl had an e.d.l thickness of approximately 5 nm in comparison with the Lytron 2503 in 0.001 M NaCl which had a thickness of greater than 30 nm. Decreasing the thickness of the e.d.l. had the effect of lowering the electrostatic repulsive forces between the particles and hence depressed the height of the primary maximum, V_{max}.

The results for the individual samples are summarised below:

Lytron 2503 in 0.001 M NaCl

The balance of DLVO and hydrodynamic forces is depicted graphically in Figure 35. The mean particle size of the latex is also plotted as a function of shear rate. It can be seen from this plot that the onset of particle aggregation occured at the shear rate predicted from the interception of of the DLVO force barrier and the hydrodynamic force curve. Hence the agreement between the experimental and theoretical shear rates was found to be excellent. The mean particle size of the aggregates was not much larger than the original latex particle size (~ 0.65 rather than 0.482 μm diameter), this was probably because the critical shear rate had only just been reached at the highest available shear rate and not many particles had aggregated.

The results are summarised in the table below:

Ionic Strength = 0.001 M
Zeta Potential = -57.1 mV

DLVO Force calculation V_{max} = 127.6 pN
DLVO Potential Energy kT_{max} = 456 kT

Critical shear rate experimental = 7.9×10^4 s^{-1}
Critical shear rate theoretical = 1.2×10^5 s^{-1}

Lytron 2503 in 0.01 M NaCl

The DLVO calculation resulted in a repulsive barrier height V_{max} of 110 pN. This result was comparable with that achieved with the Lytron 2503 in serum, which had an ionic strength of 0.011 M.

The balance of hydrodynamic and DLVO forces at various shear rates is depicted graphically in Figure 36. It can be seen that the onset of particle aggregation occured at a shear rate just prior to that predicted from the interception of the DLVO V_{max} value and the hydrodynamic force curve, giving good agreement between the experimental and theoretical critical shear rates. The mean particle size of the aggregated latex was approximately 0.85 µm at the highest shear rate ($\sim 10^5$ s^{-1}).

The results are summarised in the table below:

Ionic strength = 0.01 M
Zeta Potential = -41.0 mV

DLVO Force Calculation V_{max} = 110 pN
DLVO Potential Energy kT_{max} = 129 kT

Critical shear rate experimental = 5.6×10^4 s^{-1}
Critical shear rate theoretical = 9.1×10^4 s^{-1}

Lytron 2503 in 0.1 M NaCl

The particle size of this sample was measured prior to shearing and the mean diameter was found to approximately 0.6 μm as compared to the original particle diameter of 0.48 μm. This suggests that the repulsive force barrier had been lowered sufficiently by the addition of electrolyte for the particles to be weakly flocculated by Brownian forces.

Further shearing of the sample to approximately 10^4 s^{-1} caused irreversible aggregation of the latex into the primary minimum with the average particle size rising sharply to 1.8 um diameter. These results are depicted graphically in Figure 37.
Good agreement between the theoretical and experimental critical shear rates was found. The results are summarised below:

Ionic strength = 0.1 M
Zeta Potential = -50.8 mV

DLVO Force calculation V_{max} = 56 pN
DLVO Potential Energy kT_{max} = 17.9 kT

Critical shear rate experimental = 1 x 10^4 s^{-1}
Critical shear rate theoretical = 1.28 x 10^4 s^{-1}

8.3. Results Experiment 3

The Bohlin VOR rheogram for the latex / CMC sample is included as Figure 38. It can be seen that the viscosity of the sample has been increased by the CMC addition. The Oswald viscosity results are summarised in Table 2. The zeta potential result calculated using the relative viscosity value (see page 50) was much higher than expected (-51 mV), and when inserted into the DLVO calculation resulted in a repulsive barrier height (V_{max}) of 2700 pN (Figures 39 and 40). The hydrodynamic force curve obtained for this sample is attached as Figure 41.

Subsequent shearing of the latex/CMC sample and measurement of the resultant particle size showed that no aggregation had occurred.

Discussions with with Prof. R. Ottewill shed some light on this result. It was thought that the microscopic viscosity of the latex/CMC solution should have been measured rather than the macroscopic viscosity. This macroscopic viscosity when

incorporated into the Helmholtz - Smoluchowski equation led to the erronously high value. The CMC was also thought to complicate the situation by possibly adsorbing onto the latex surface and sterically hindering the particle aggregation. This complex situation is outside the scope of this project and more work would be necessary to acertain whether CMC adsorbs onto the latex surface and the magnitude of steric effects.

9. Conclusions

1. Lytron 2503 was found to be a fairly monodisperse polystyrene latex with a particle diameter of 0.482 μm. The emulsifier and residual salts in the serum were removed successfully using the technique of diafiltration, and the sodium and potassium counter ions were replaced with hydrogen ions by washing with dilute acid. The surface charge was determined using conductometric titration with NaOH and was found to be 8.50 μC cm^{-2} due to carboxyl groups and 4.46 μC cm^{-2} due to the sulphate groups. These values are typical of a paper coating latex.

2. The Lytron 2503 as received appears to be stable at shear rates up to 1.24×10^{-5} s^{-1} as measured on the Bohlin VOR with a tapered plug geometry.

3. Addition of a 1:1 electrolyte to decrease the thickness of the electrical double layer and hence the repulsive forces between particles, enabled the maximum shear rates obtainable with the Bohlin rheometer to cause the latex particles to aggregate. The total force and energy curves determined for this latex in electrolyte solutions were in agreement with previous work on model latices (11).

4. Comparison of the DLVO repulsive forces and hydrodynamic forces incurred by shearing, proved to be a successful method for predicting the onset of shear induced aggregation. The theoretical critical shear rates compared well with those found experimentally.

This project has proved valuable as a basic study of colloid stability and has led to a greater understanding of the factors which influence it. The comparison of experimental and theoretical critical shear rates has shown to be a suitable method to study shear induced aggregation of paper coating latices.

10. Further work

Further work on the topic of shear induced aggregation should include the following:

1. This study could be extended to investigate the shear induced aggregation of kaolin and calcium carbonate pigments, using close cut fractions of a suitable size (<< 2 um) for PCS to be reliably used. It would then be possible to introduce a latex in order to study shear induced aggregation of a coating colour.

2. The effect of particle size on the aggregation of a colloid could be determined using a series of monodisperse latices with varing particle sizes (e.g. 0.2 um, 0.5 um, 0.7 um and 1.0 um diameter). Theoretically an increase in particle diameter should lower the critical shear rate (equation 26)

3. Methods of increasing the viscosity of a latex suspension should also be investigated. A viscosifing agent which dose not adsorb and sterically stabilize the system is necessary. A concentrated sucrose solution could be used for this purpose. An increase in viscosity should theoretically reduce the critical shear rate by increasing the hydrodynamic forces.

4. The possible adsorption of CMC onto the latex surface is an area which should be investigated further using a technique described by J.C. Husband (26).

11. References

(1) Luckham P. F., Vincent B., Colloids and Surface, 6, 1983, 83-95, Elsevier Scientific Publishing Co., Amsterdam,

(2) Whalen - Shaw M., Sheehan, J.G., Tappi Journal, May 1990, Atlanta.

(3) Stamberger, P., J. Colloid Sci. 17, 146 (1962)

(4) Zeichner, G.R., Schowalter W.R., J. Colloid Interface Sci. 71 , 237 (1979)

(5) Verwey, E.J.W., and Overbeek, J., Theory of the Stability of Lyophobic Colloids Amsterdam Elsevier, (1948)

Derjaguin, B. V., Landau, L., Acta physicochim URSS 10:333 (1939)

(6) Goren, S.L., J. Colloid Interface Sci, 36 , 94 (1971)

(7) Bangs, L.B.,"Uniform Latex Particles", Seradyn p5-8

(8) El-Aasser. M.S., "Scientific Methods for the Study of Polymer Colloids and their Applications" p1-5, Kluwer Academic Publishing, Netherlands.

(9) Basset D., Hamielec A., "Emulsion Polymers and Emulsion Polymerisation", ACS Symposium 165 (1981), p61-84.

(10) Blackley D.C., "Science and Technology of Polymer Colloids", Volume 1, 1983, Kluwer Academic Publishing Group, Dordrecht, Netherlands, P203-219

(11) Buscall, R., Corporate Colloid Science Grp. ICI Plc. "Science and Technology of Polymer Colloids", 1983, Kluwer Academic Publishers Group, Netherlands, p279 - 291.

(12) de Boer, J.H., Trans Faraday Soc., 32 , 21 (1936)

(13) Ottewill, R.H., in "Scientific methods for the Study of Polymer Colloids and Their Applications", Ed. Candau and Ottewill, 1988, p135, Kluwer Academic, Dordrecht.

(14) Von Smoluchowski, N., Z. Physik Chem. 92 129 (1917)

(15) Zeichner, G.R., Schowalter, W.R., A.I.Ch.E.J., 23 , 243 (1977)

(16) C.J. Pouchert, The Aldrich Library of Infra Red Spectra, Edition 3. Aldrich Chemical Co., Milwaukee, Wisconsin, 1981

(17) Vanderhoff, J.W., Van Den Hul, H.J., Tausk, R.J.M., Overbeek, J.T.H.G., " The preparation of monodisperse latices with well characterised surfaces " p15 -43. "Clean surfaces", Marcel Dekker, INC. 1970, New York.

(18) El-Aasser M.S., "Science and Technology of Polymer Colloids", Volume 2, 1983, Kluwer Academic Publishers, Netherlands.

(19) Almed, S.M., El-Asser, M.S., Pauli, G.H., Poehlein, G.W., Vanderhoff, J.W., J. Colloid Interface Sci. 73 388 (1980).

(20) Warren Springs Laboratories: Viscometers (UK) Ltd. User manual p4 - 9.

(21) Everett, D.H., in RSC Paperback "Basic Principles of Colloid Science" p104 - 106. RSC Publications, London, 1988.

(22) Gane, P.A.C., - Internal Research Report 8301/1

(23) Rogan, K., Internal Research Report

(24) Helmholtz, H., Ann. Physik , 7 , 337 (1879).

(25) Smoluchowski, M., Bull. Acad. Sci. Cracovie, 182 (1903).

(26) Husband. J.C., Gates, M.S., Internal Report.

General Reading

(27) Dittgen, M., Zosel, B., Colloid Polym. Sci., 269 : 259 - 263 (1991).

(28) Ottewill, R.H., Goodwin, J.W., J. Chem. Soc. Faraday Trans., 1991, 87 (3), 357 - 369.

(29) Davies, R.M., Tappi Journal May 1987 p99 - 104.

(30) Lee, D. I., Tappi Conference Procceedings, 1972, 201 - 231

12. Acknowledgements

I would like to thank the following people for their guidance and assistance:

1. Mr. J.C Husband, ECCI, for supervising the project and for giving me the original idea.

2. Dr.G.P. Matthews and Prof. Bancroft, PSW, for their supervision of this project.

3. Prof. R.H. Ottewill for helpful discussions.

4. JPKettle, D Sturge, K Logan

BOHLIN RHEOMETER SYSTEM *E. C. C. RESEARCH AND DEVELOPMENT*

Viscometry test

1991-01-20 16: 28: 58

Figure 24. Lytron 2503 (as received)

Viscosity

No A zero

TP20: 1 gap 0.10 mm
92.83 gcm 1

CDt 10.0 It 10.0
No of M 1
MI 10 s

T 19.9 - 20.2 C
R 2.28 - 11.65 %

JSP25032

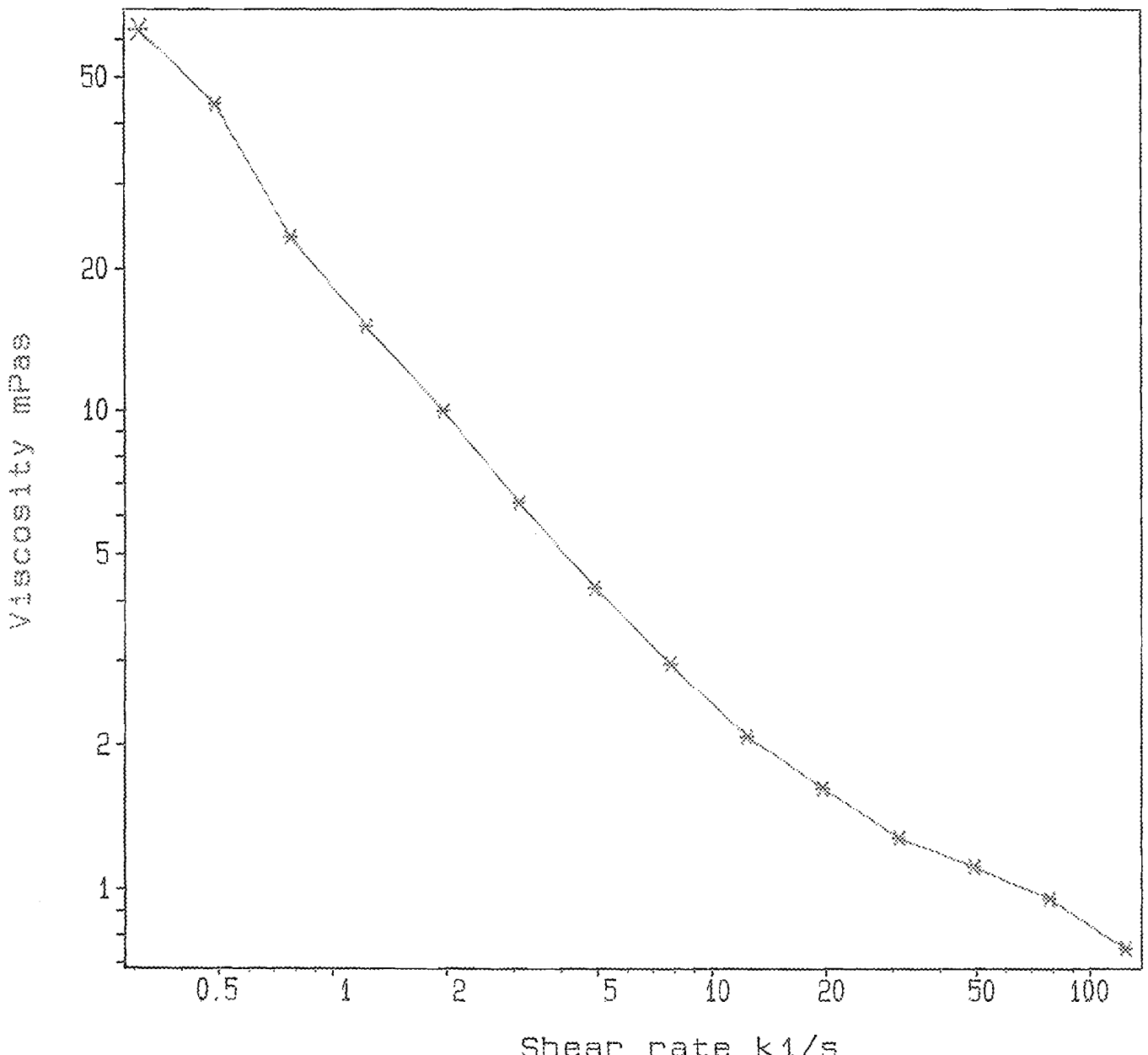

Figure 25 Lytron 2503 Particle Diameter After Shearing

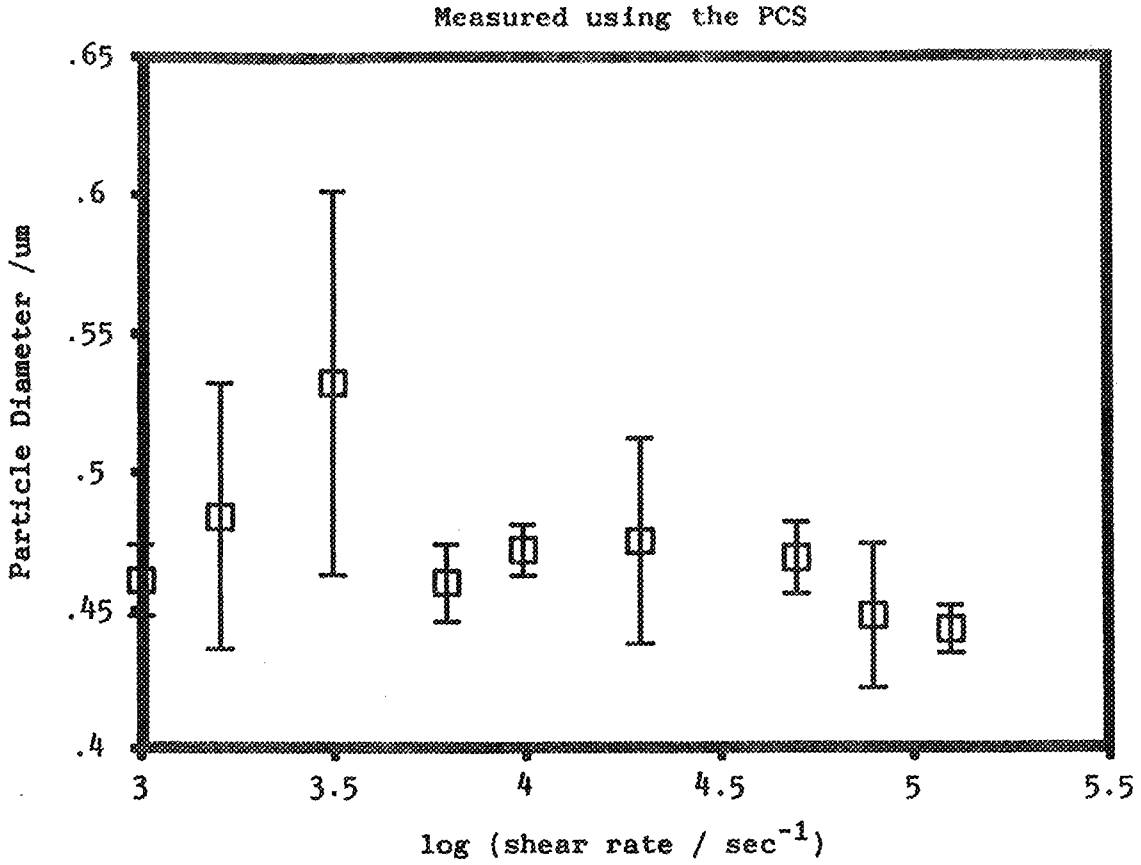

Figure 26 Lytron 2503 Particle Diameter when Sheared for Varing Times

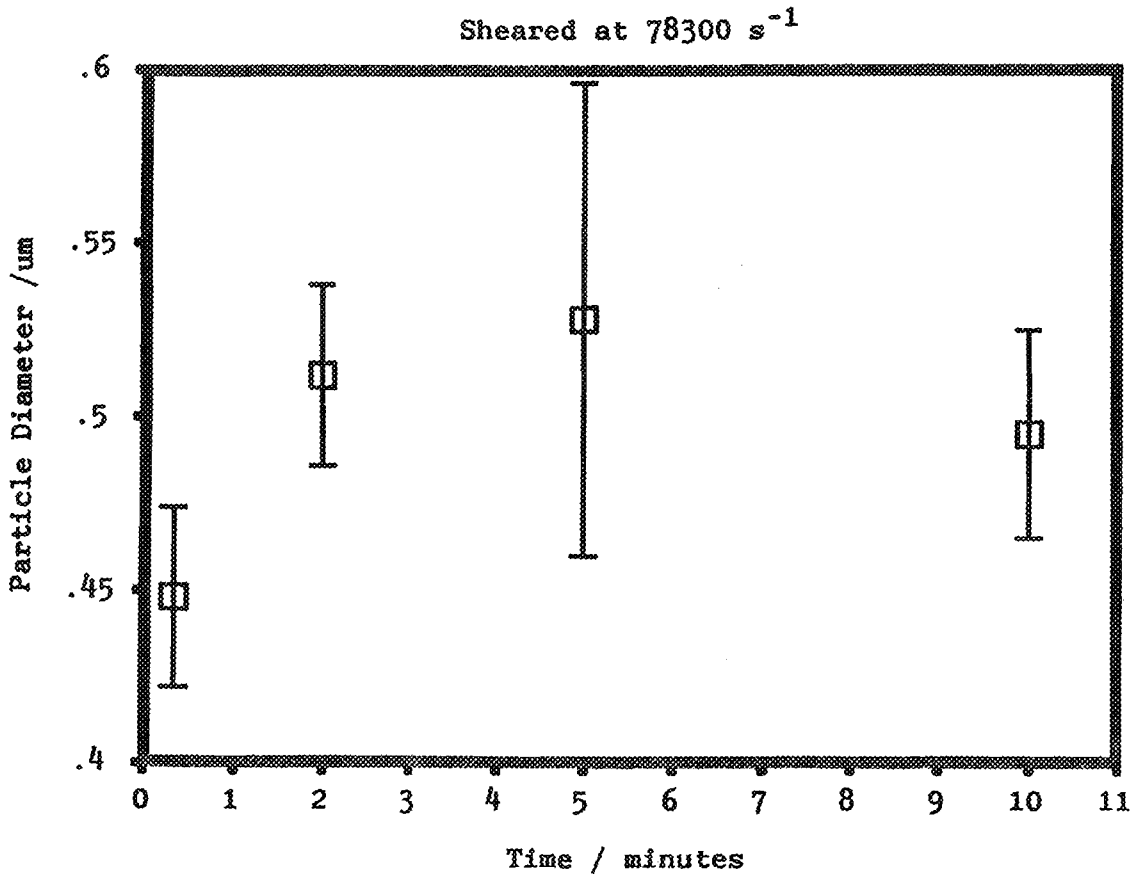

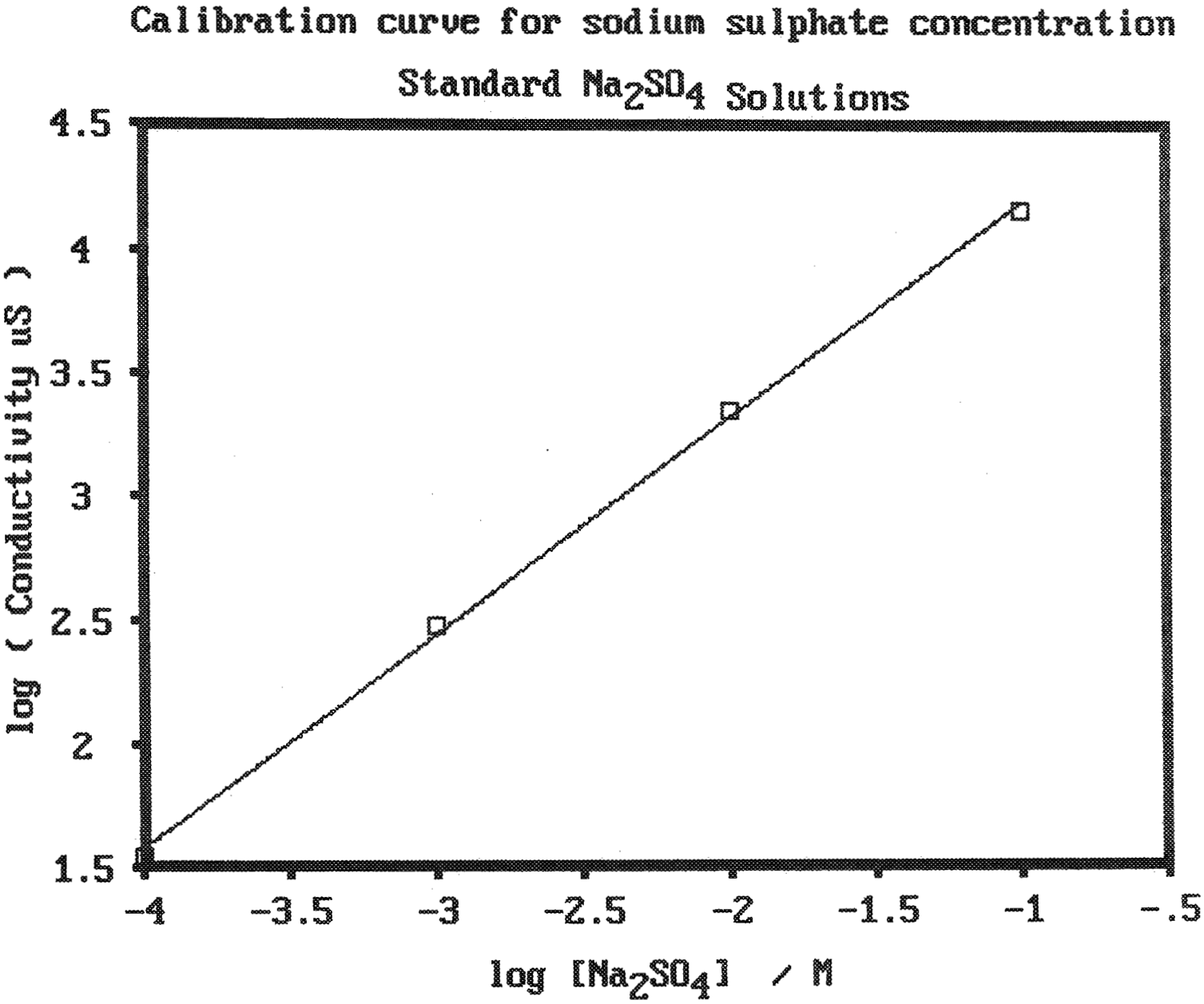
Calibration curve for sodium sulphate concentration
Standard Na_2SO_4 Solutions
log (Conductivity uS)
4.5
4
3.5
3
2.5
2
1.5
-4
-3.5
-3
-2.5
-2
-1.5
-1
-.5
log [Na_2SO_4] / M

Figure 28

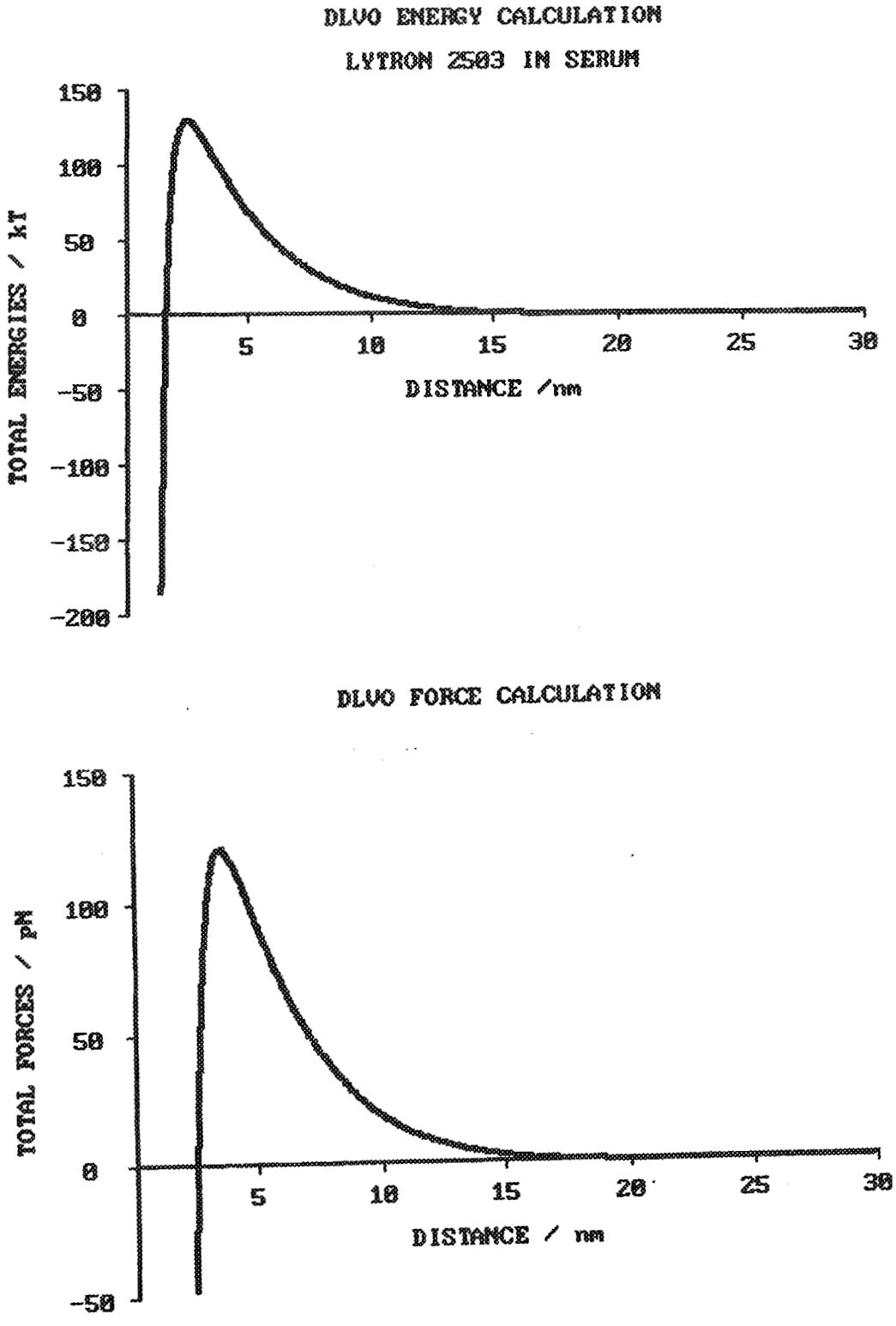
DLVO ENERGY CALCULATION
LYTRON 2503 IN SERUM
TOTAL ENERGIES / kT
150
100
50
0
-50
-100
-150
-200
5
10
15
20
25
30
DISTANCE /nm
DLVO FORCE CALCULATION
TOTAL FORCES / pN
150
100
50
0
-50
5
10
15
20
25
30
DISTANCE / nm

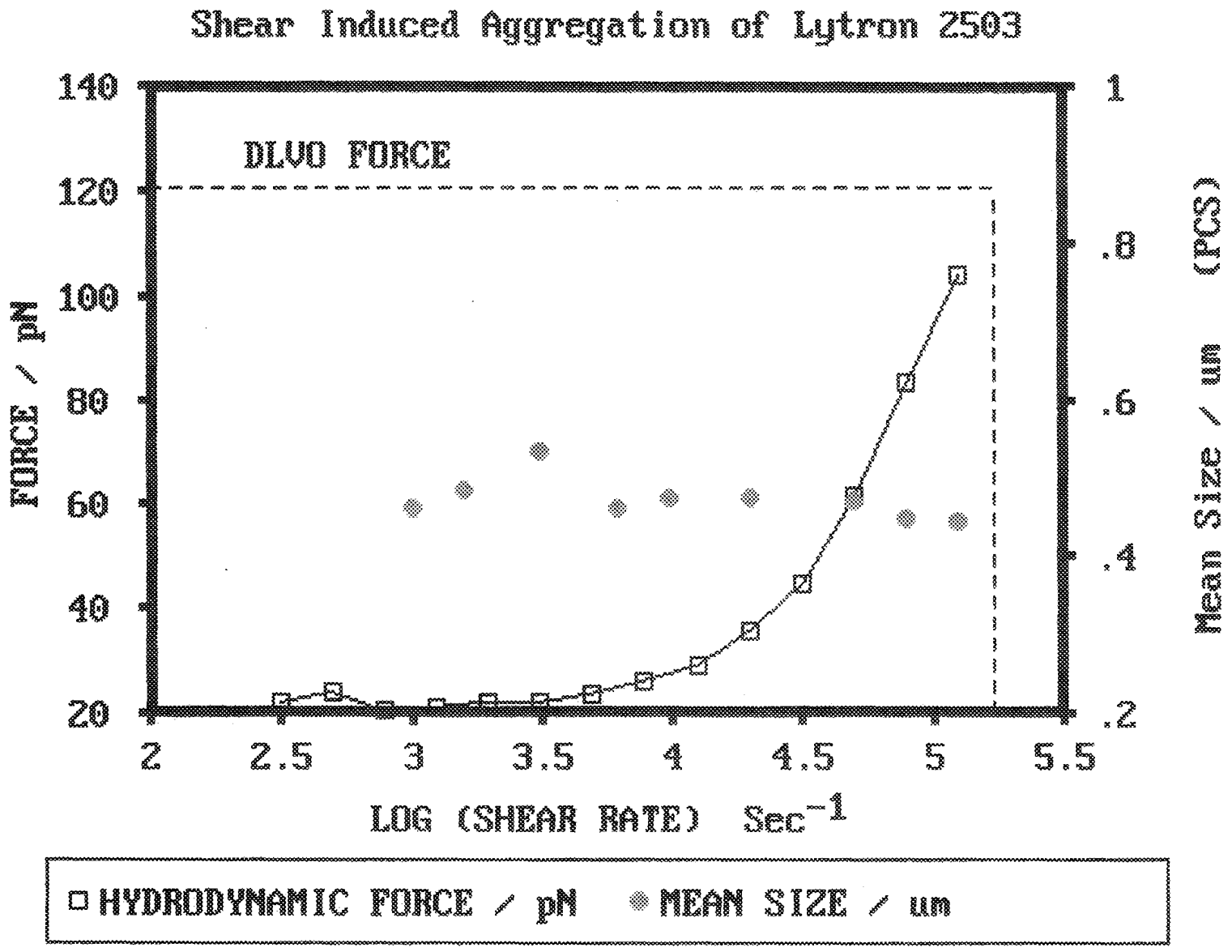
Shear Induced Aggregation of Lytron 2503
DLVO FORCE
FORCE / pN
Mean Size / um (PCS)
140
120
100
80
60
40
20
1
.8
.6
.4
.2
2
2.5
3
3.5
4
4.5
5
5.5
LOG (SHEAR RATE) Sec-1
HYDRODYNAMIC FORCE / pN
MEAN SIZE / um

Figure 29

BOHLIN RHEOMETER SYSTEM *E.C.C. RESEARCH AND DEVELOPMENT*

Viscometry test

1991-04-25 14:47:35

Figure 30. Lytron 2503 in 0.001M NaCl

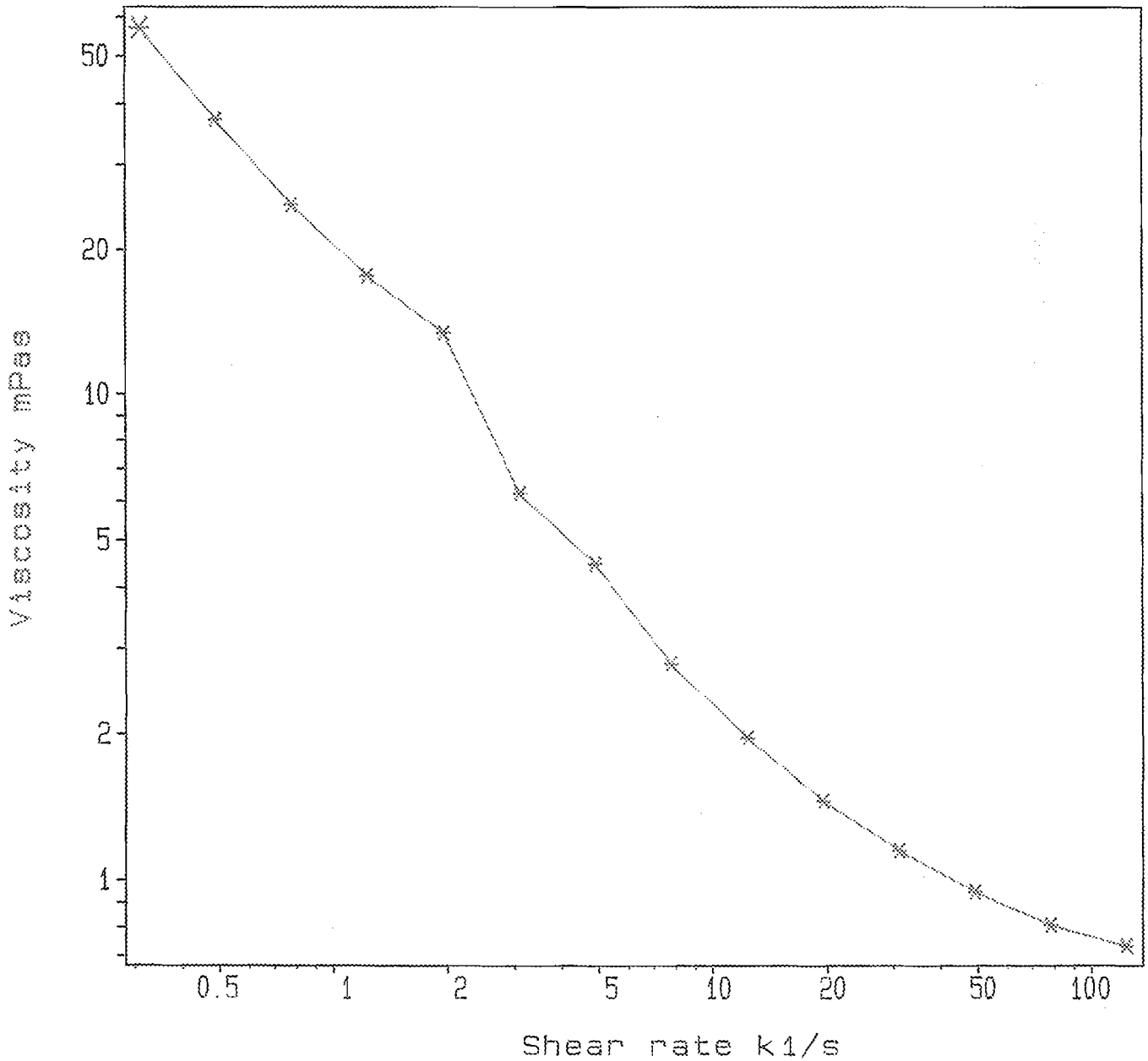

No A zero

TP20: 1 gap 0.10 mm
92.83 gcm 1

CDt 10.0 It 10.0
No of M 1
MI 10 s

T 19.9 - 20.2 C
R 2.23 - 11.42 %

001NACL1

BOHLIN RHEOMETER SYSTEM *E. C. C. RESEARCH AND DEVELOPMENT*

Viscometry test

1991-04-25 14: 21: 41

Figure 31. Lytron 2503 in 0.01M NaCl

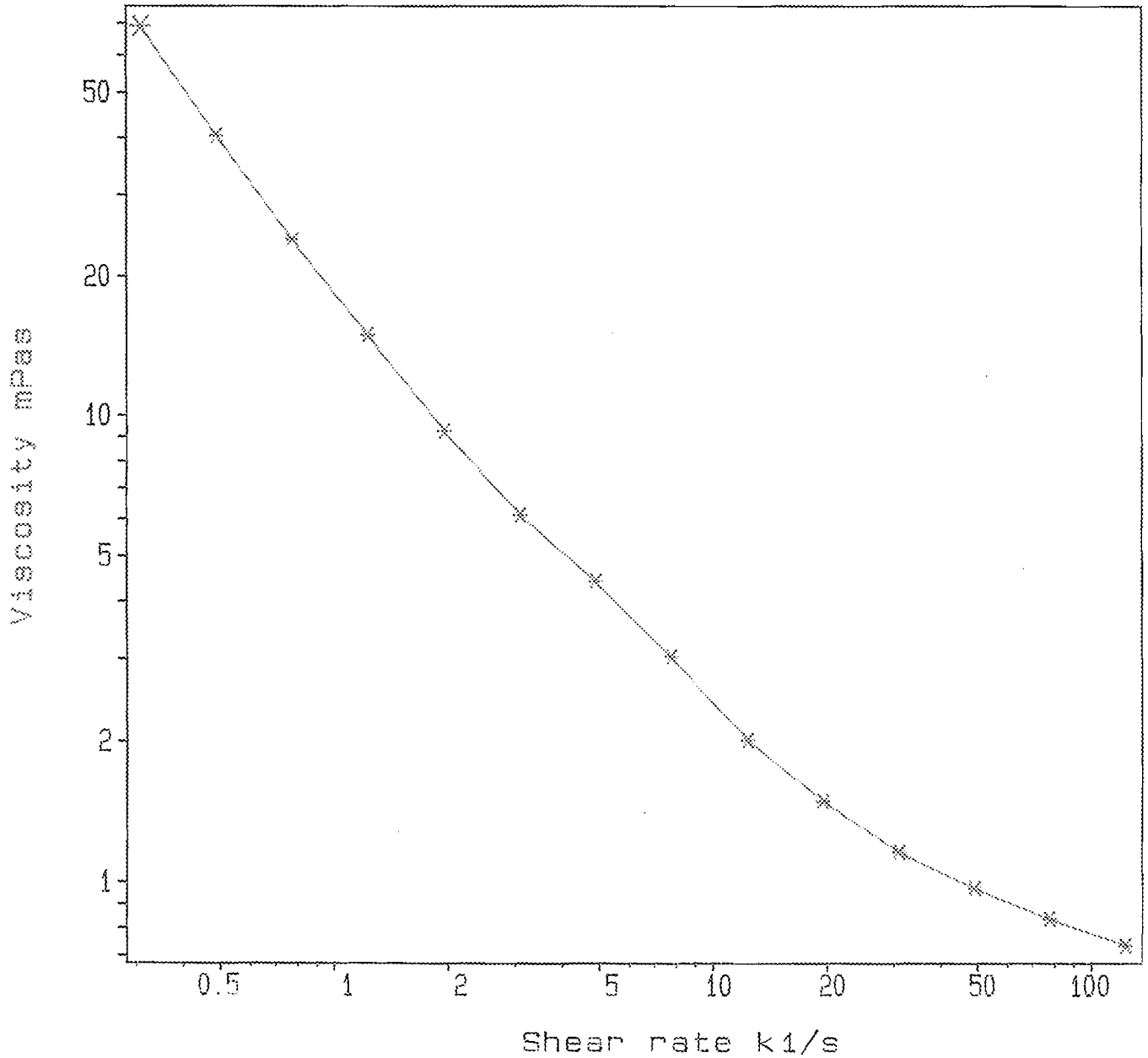

No A zero

TP20: 1 gap 0.10 mm
92.83 gcm 1

CDt 10.0 It 10.0
No of M 1
MI 10 s

T 19.9 - 20.1 C
R 2.29 - 11.47 %

01NACL3

BOHLIN RHEOMETER SYSTEM *E.C.C. RESEARCH AND DEVELOPMENT*

Viscometry test

1991-05-01 16:03:55

Figure 32. Lytron 2503 in 0.1M NaCl

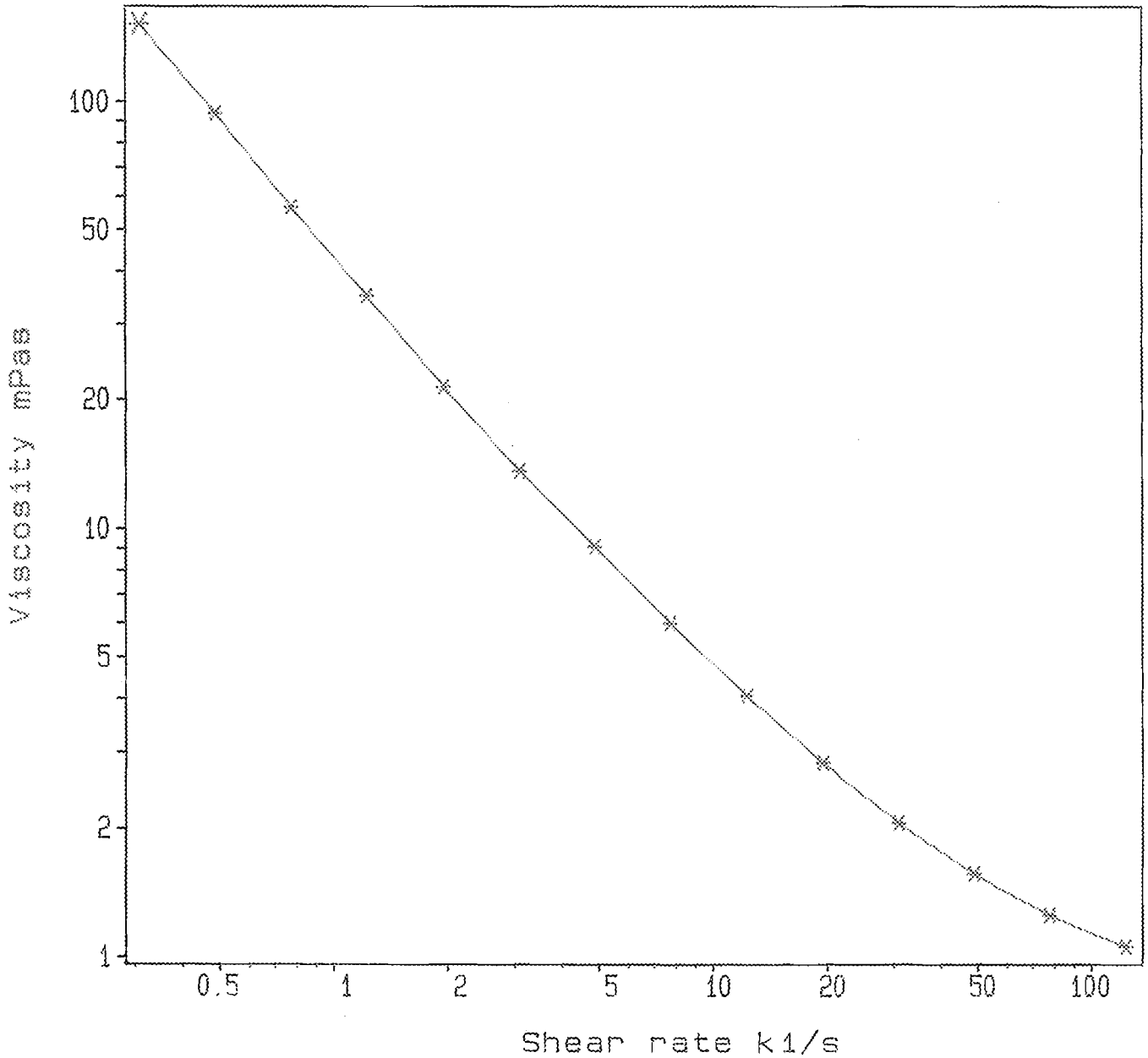

No A zero

TP20: 1 gap 0.10 mm
288.50 gcm 1

CDt 10.0 It 10.0
No of M 1
MI 10 s

T 19.9 - 20.1 C
R 1.70 - 5.29 %

1NACL2

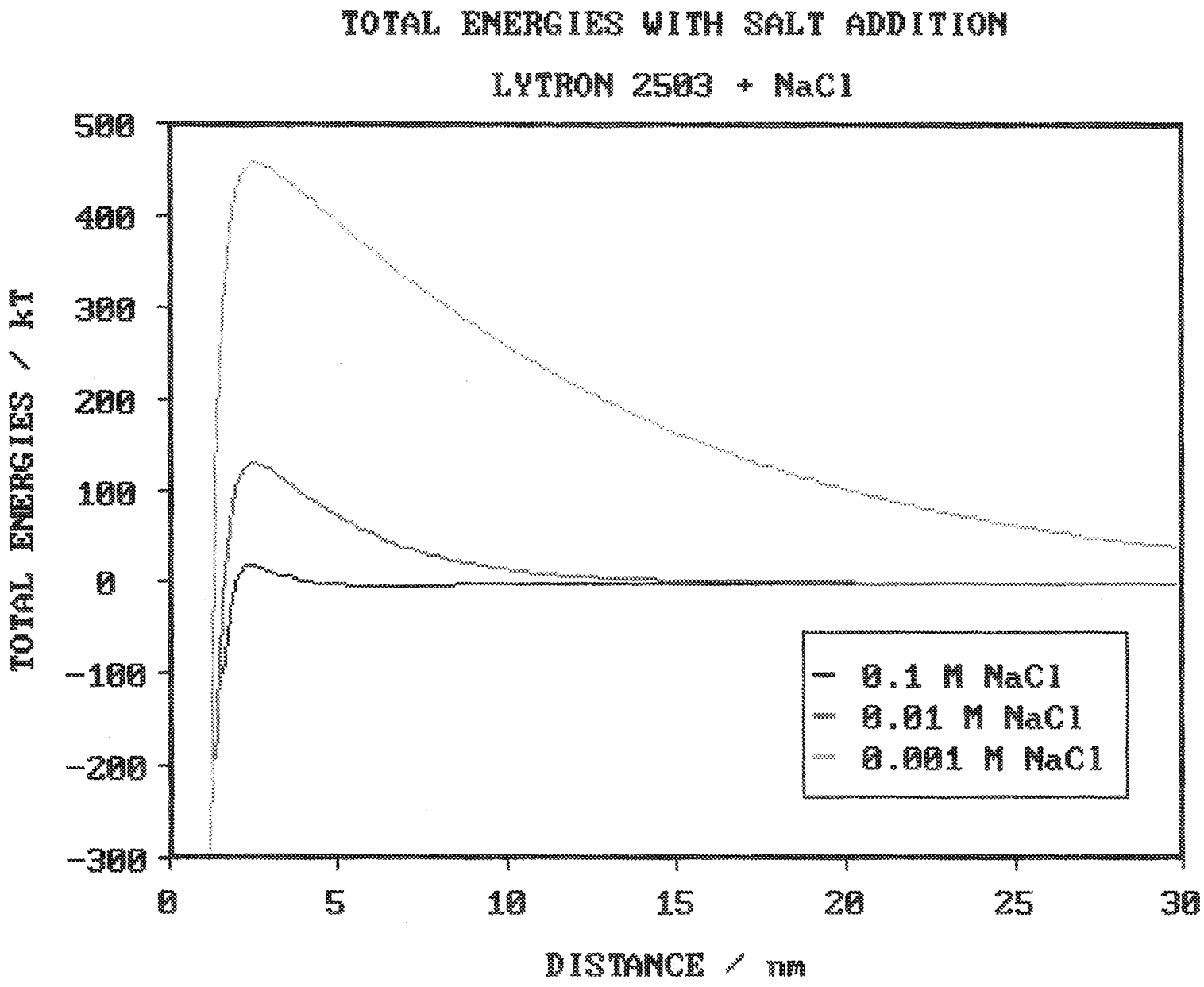
TOTAL ENERGIES WITH SALT ADDITION
LYTRON 2503 + NaCl
TOTAL ENERGIES / kT
500
400
300
200
100
0
-100
-200
-300
0
5
10
15
20
25
30
DISTANCE / nm
0.1 M NaCl
0.01 M NaCl
0.001 M NaCl

Figure 33

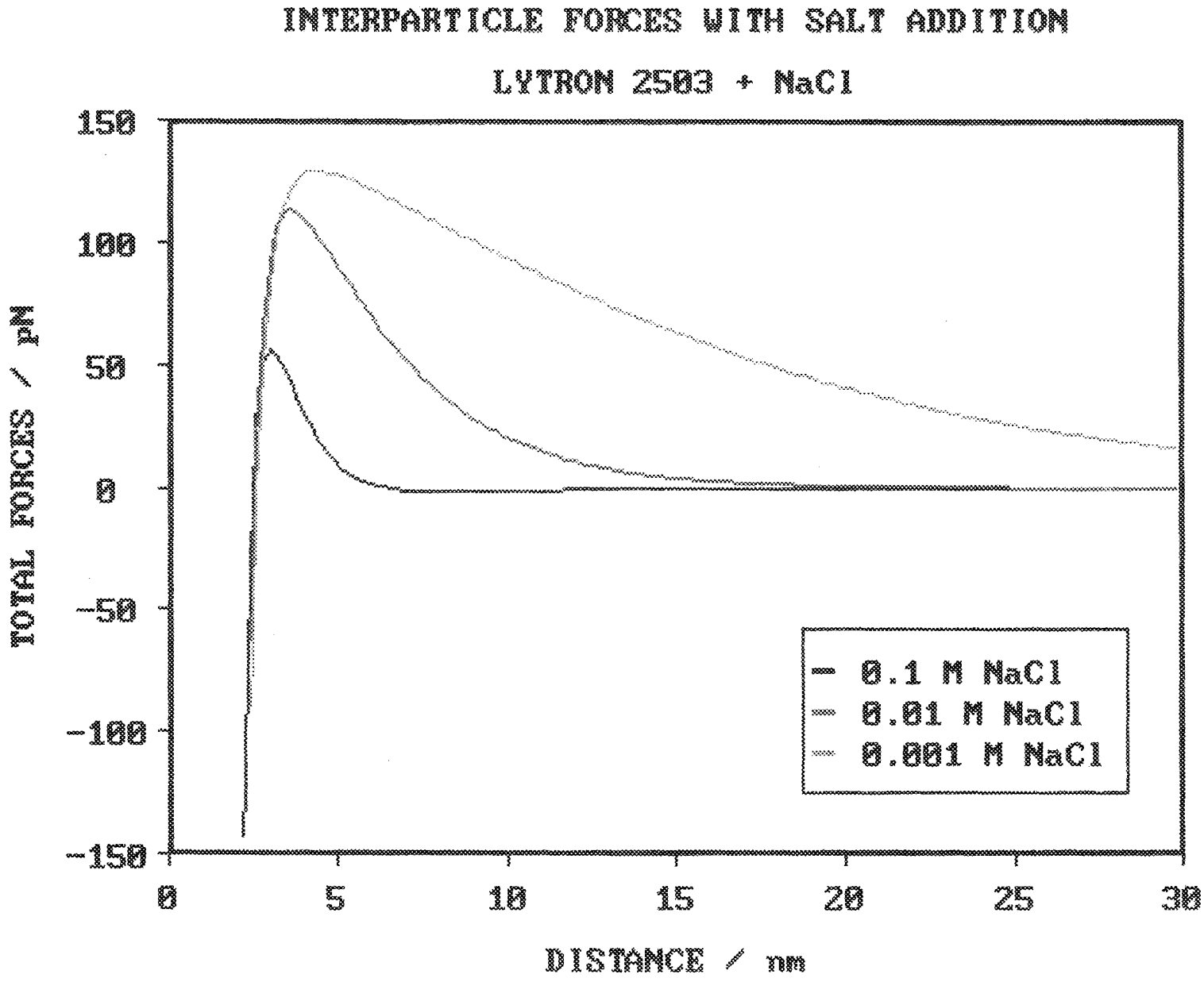
INTERPARTICLE FORCES WITH SALT ADDITION
LYTRON 2503 + NaCl
TOTAL FORCES / pN
150
100
50
0
-50
-100
-150
0
5
10
15
20
25
30
DISTANCE / nm
0.1 M NaCl
0.01 M NaCl
0.001 M NaCl

Figure 34

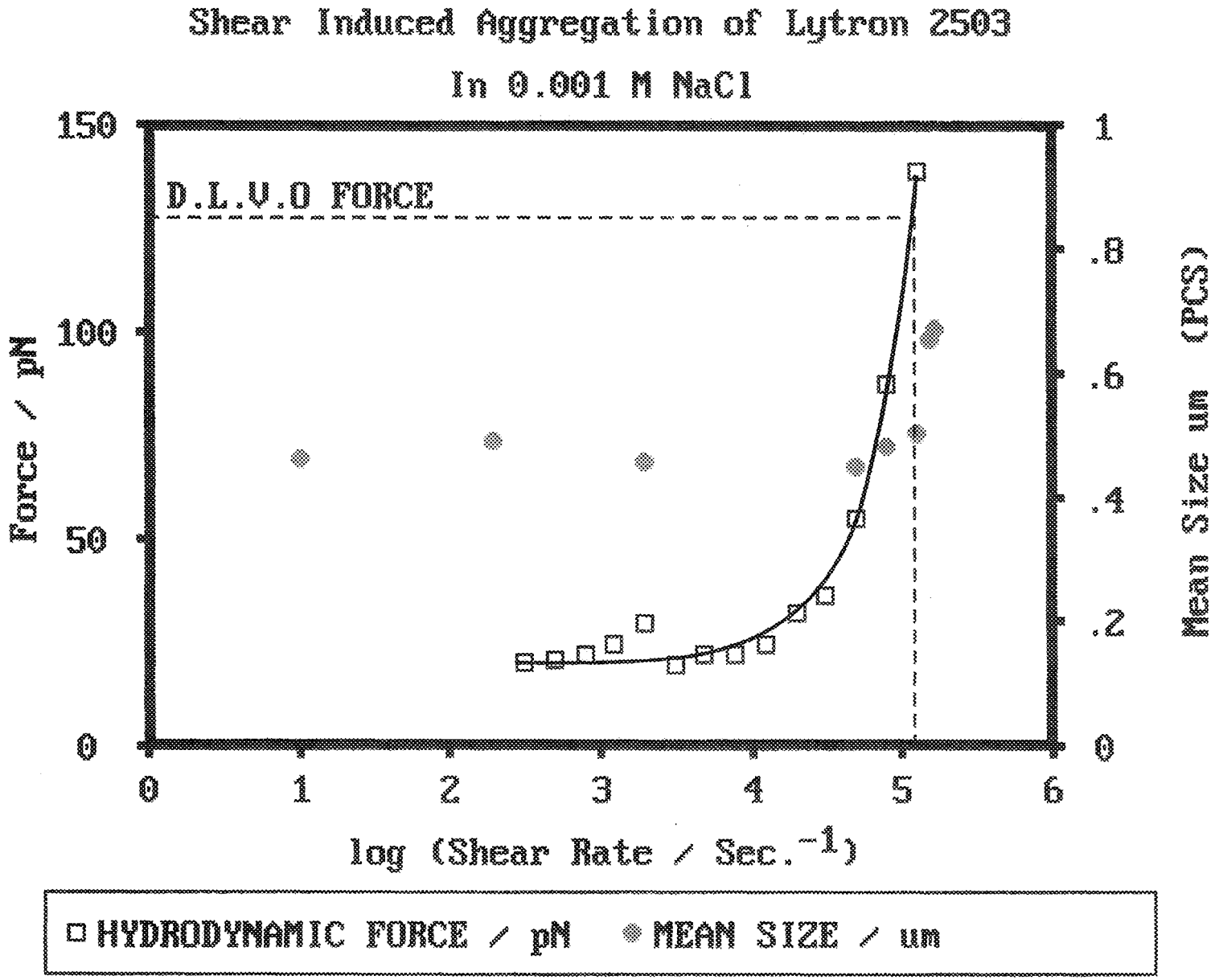
Shear Induced Aggregation of Lytron 2503
In 0.001 M NaCl
D.L.V.O FORCE
Force / pN
Mean Size um (PCS)
150
100
50
0
1
.8
.6
.4
.2
0
0
1
2
3
4
5
6
log (Shear Rate / Sec.-1)
HYDRODYNAMIC FORCE / pN
MEAN SIZE / um

Figure 35

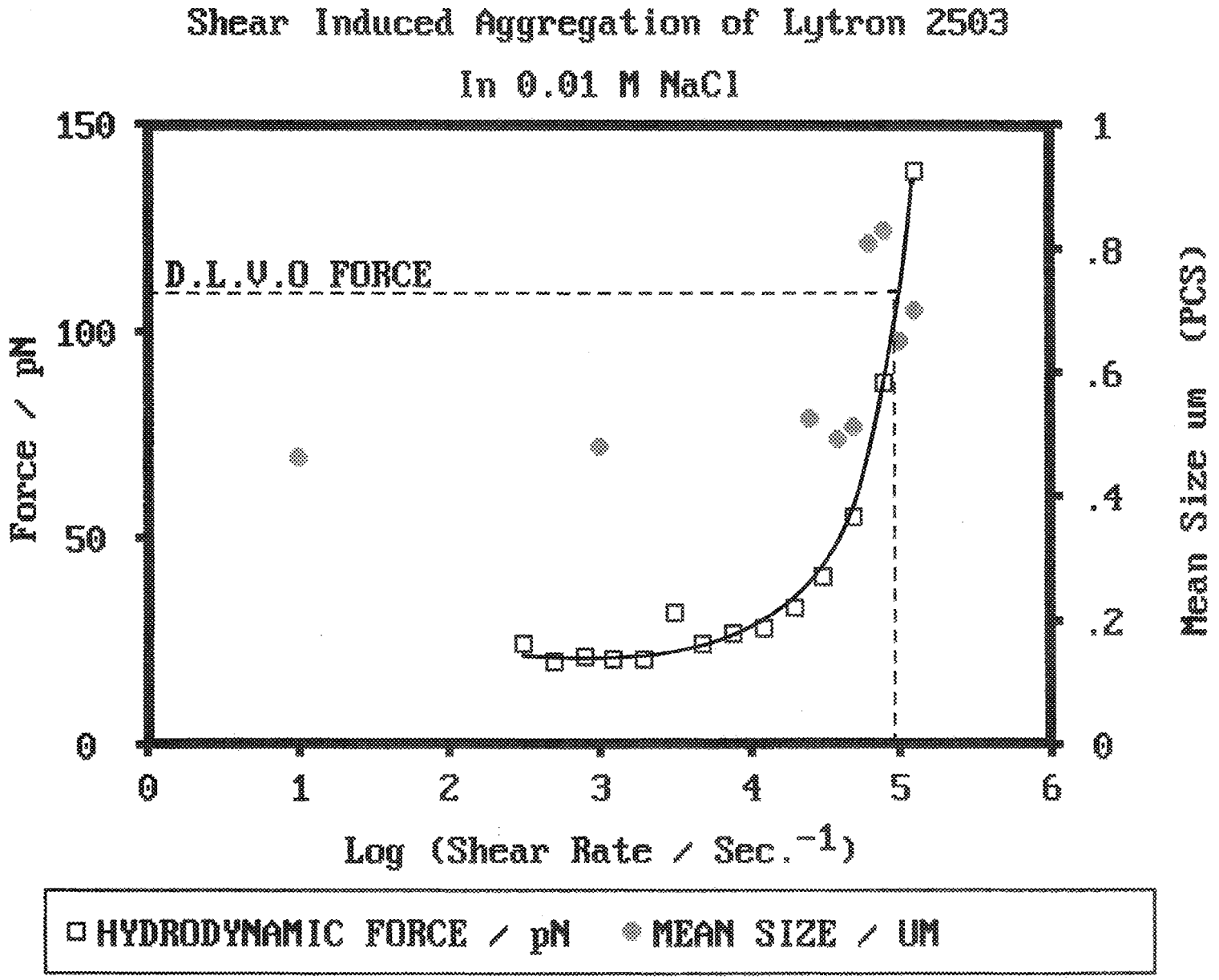
Shear Induced Aggregation of Lytron 2503
In 0.01 M NaCl
150
100
50
0
D.L.V.O FORCE
Force / pN
1
.8
.6
.4
.2
0
Mean Size um (PCS)
0
1
2
3
4
5
6
Log (Shear Rate / Sec.$^{-1}$)
HYDRODYNAMIC FORCE / pN
MEAN SIZE / UM

Figure 36

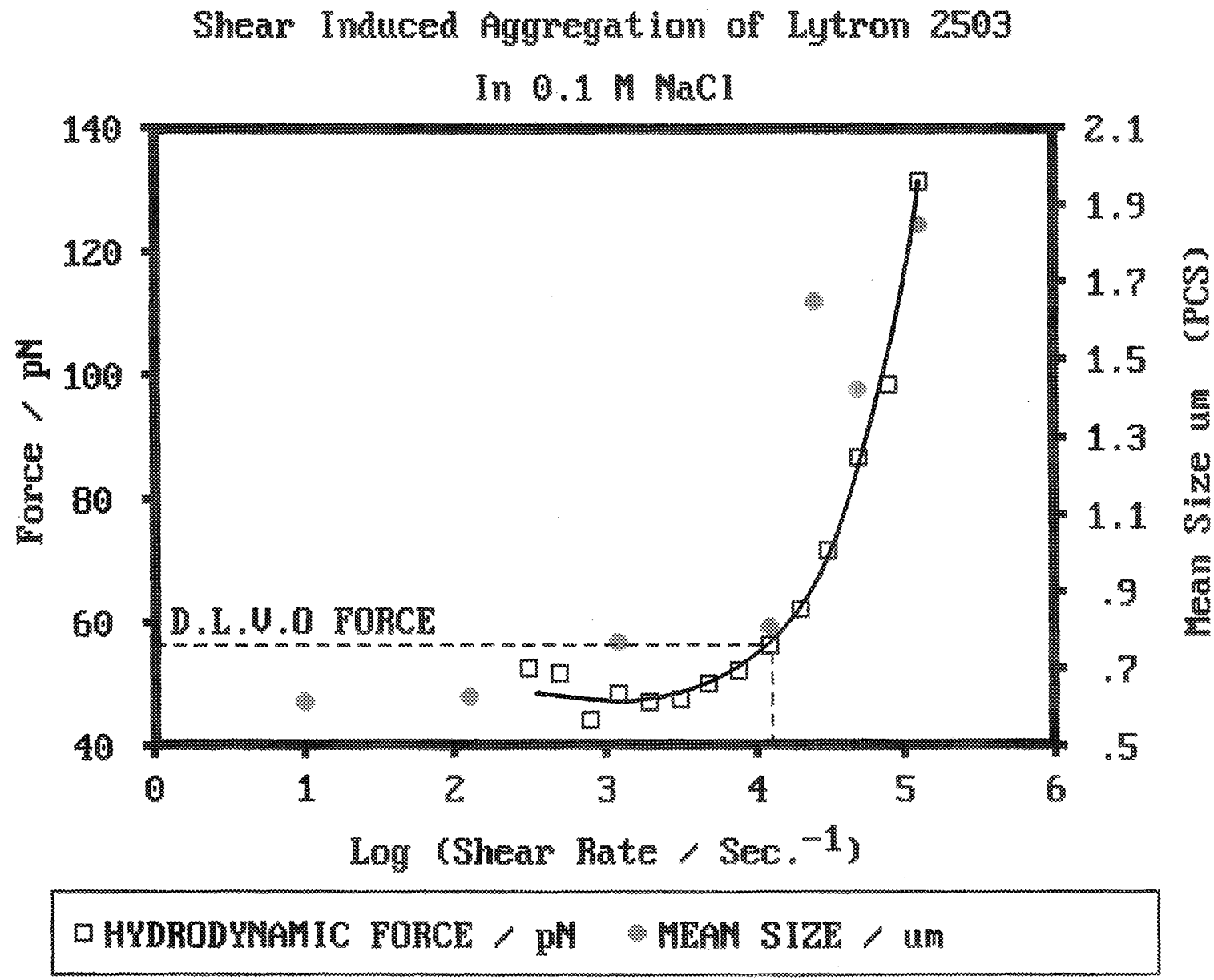
Shear Induced Aggregation of Lytron 2503
In 0.1 M NaCl
Force / pN
Mean Size um (PCS)
D.L.V.O FORCE
Log (Shear Rate / Sec.$^{-1}$)
HYDRODYNAMIC FORCE / pN
MEAN SIZE / um

Figure 37

BOHLIN RHEOMETER SYSTEM *E.C.C. RESEARCH AND DEVELOPMENT*

Viscometry test

1991-02-14 15:57:10

lytron 2503 with cmc 10%

- Viscosity

No A zero

TP20: 1 gap 1.00 mm
288.50 gcm 1

CDt 10.0 It 10.0
No of M 1
MI 20 s

T 19.9 - 20.1 C
R 4.47 - 29.60 %

LMID1

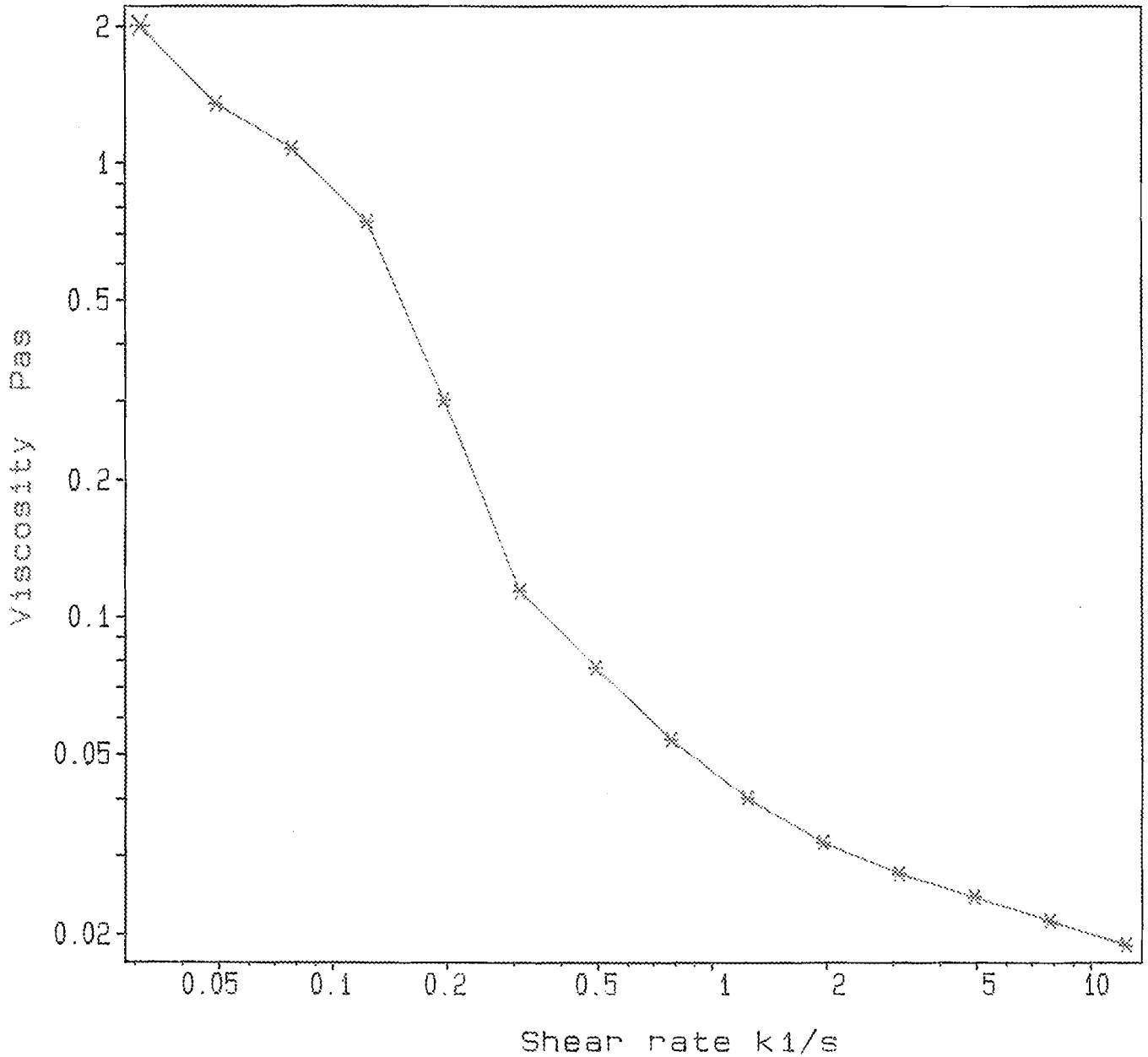

Figure 38

OSWALD VISCOSITY RESULTS

WATER (SECONDS)	7MID (SECONDS)
12.65	47.08
12.51	47.51
12.34	47.67
12.52	47.51
12.57	47.53
12.41	47.68
12.58	47.54
12.40	47.45
12.45	47.60
12.57	47.52

AVERAGE VALUE FOR WATER = 12.5 s
AVERAGE VALUE FOR 7MID = 47.51 s

RELATIVE VISCOSITY = 47.51 / 12.5 =3.801

DLVO FORCE CALCULATION

LYTRON 2503 IN SERUM WITH ADDED CMC

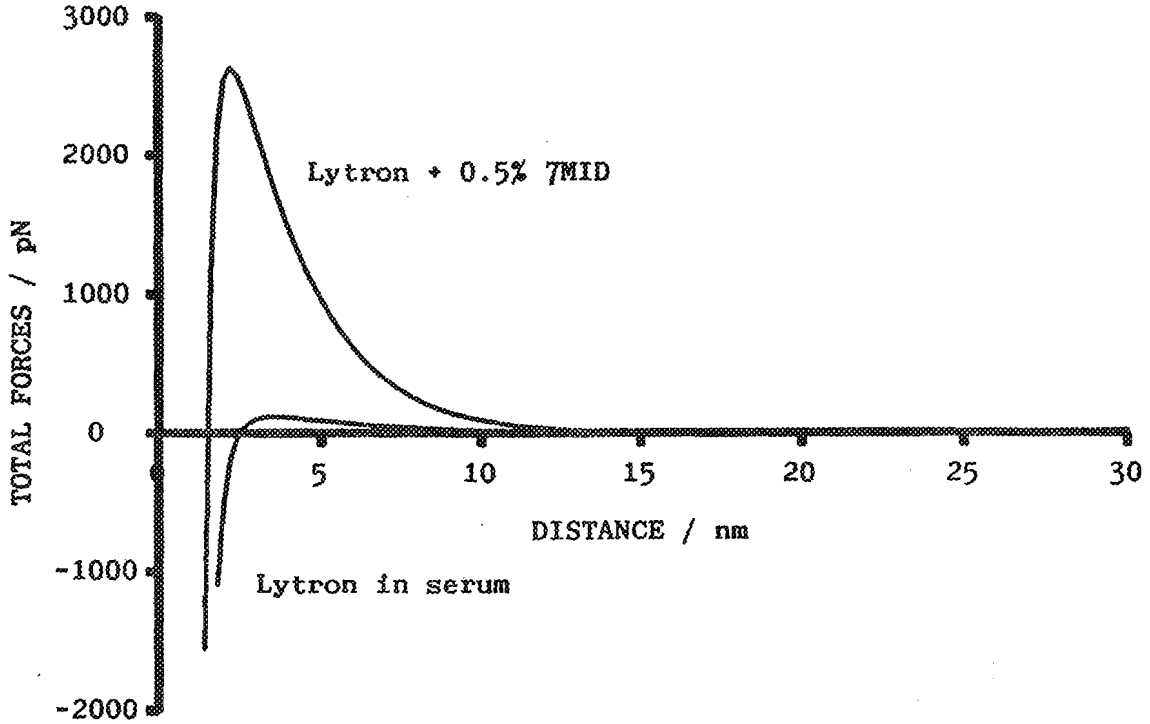

DLVO ENERGY CALCULATION

Figure 40

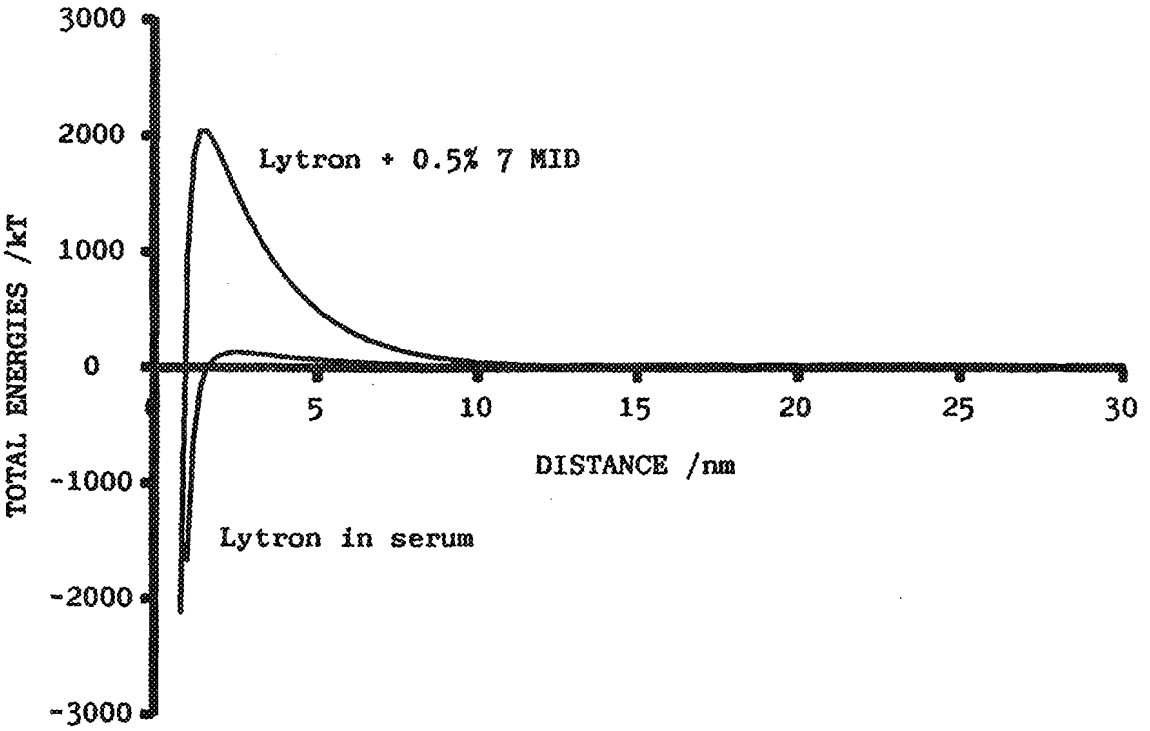

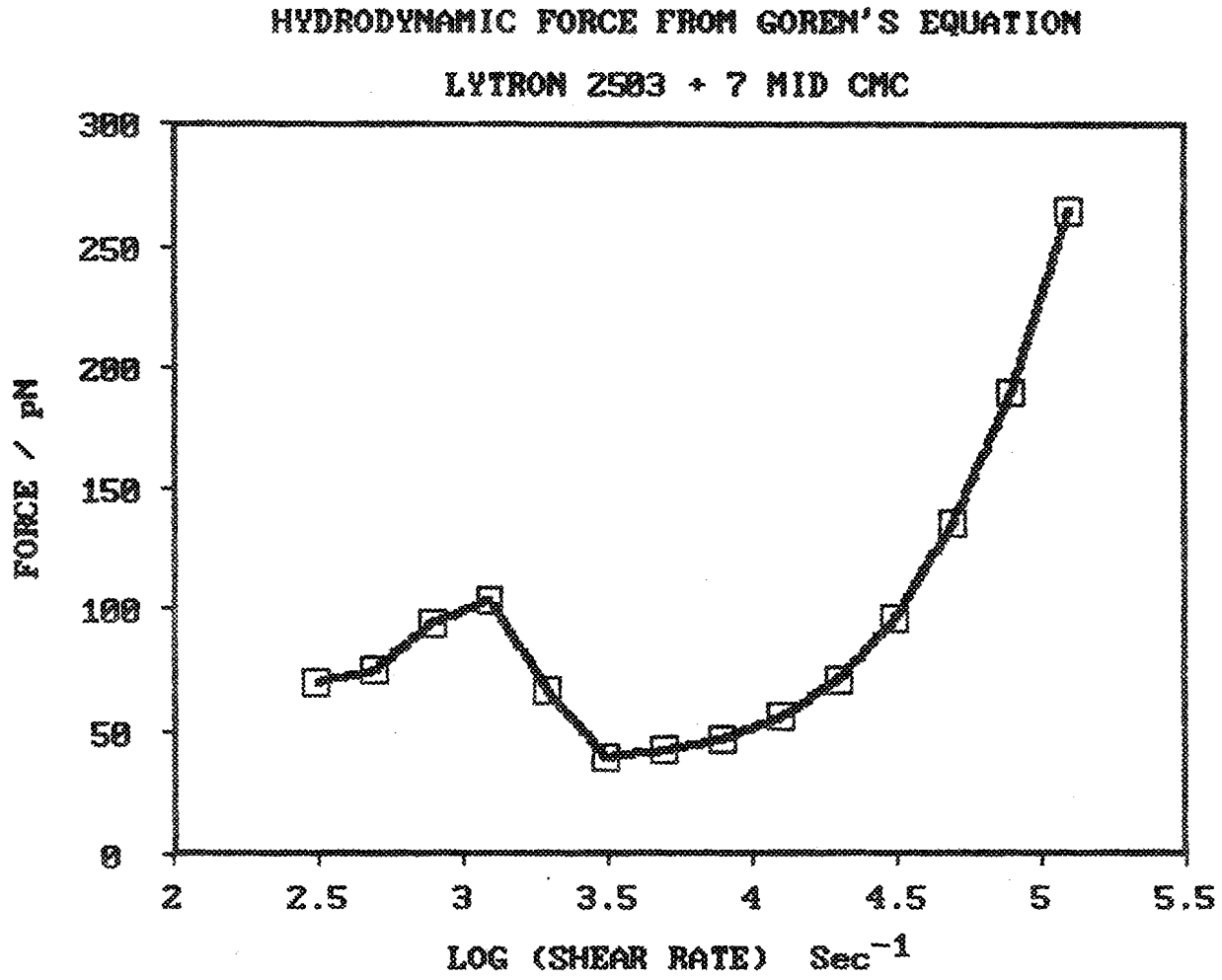
HYDRODYNAMIC FORCE FROM GOREN'S EQUATION
LYTRON 2503 + 7 MID CMC
FORCE / pN
300
250
200
150
100
50
0
2
2.5
3
3.5
4
4.5
5
5.5
LOG (SHEAR RATE) Sec^{-1}

Figure 41